Hsp47 Promotes Biogenesis of Multi-subunit Neuroreceptors in the Endoplasmic Reticulum

Ya-Juan Wang,[1,4] Xiao-Jing Di,[1,4] Dong-Yun Han,[1] Raad Nashmi,[2]

Brandon J. Henderson,[3] Fraser J. Moss,[1] Ting-Wei Mu[1,*]

[1]Department of Physiology and Biophysics, Case Western Reserve University School of Medicine, 10900 Euclid Ave, Cleveland, Ohio 44106, USA.

[2]Department of Biology, University of Victoria, Victoria, BC, V8W 3N5, Canada.

[3]Department of Biomedical Sciences, Joan C. Edwards School of Medicine at Marshall University, 1700 3rd Ave, Huntington, WV 25703-1104, USA.

[4]These authors contributed equally to this work.

[*]To whom correspondence should be addressed.

Telephone: 216-368-0750; Fax: 216-368-5586; E-mail: tingwei.mu@case.edu

Running Title: Hsp47 promotes multi-subunit ion channel proteostasis.

Keywords: Hsp47, folding, assembly, trafficking, $GABA_A$ receptors, nAChRs, proteostasis, epilepsy

Highlights

- Hsp47 positively regulates the functional surface expression of endogenous $GABA_A$ receptors.
- Hsp47 acts after BiP and preferentially binds the folded conformation of $GABA_A$ receptors.
- Hsp47 promotes the subunit-subunit assembly of $GABA_A$ receptors.
- Hsp47 plays a critical and general role in the maturation of multi-subunit neuroreceptors.

ABSTRACT

Protein homeostasis (proteostasis) deficiency is recognized as a contributing factor to many neurodegenerative, neurological, and metabolic diseases. However, how the proteostasis network orchestrates the folding and assembly of multi-subunit membrane proteins is not completely understood. In this investigation, we focus on characterizing the biogenesis pathway of a multi-subunit neuroreceptor, the γ-aminobutyric acid type A ($GABA_A$) receptor. Previous proteomics studies identified Hsp47 (Gene: *SERPINH1*), a heat shock protein in the endoplasmic reticulum lumen, as the most enriched $GABA_A$ receptor-interacting chaperone. Here, we show that Hsp47 enhances neuronal $GABA_A$ receptor functional surface expression, acting after Binding immunoglobulin Protein (BiP), to preferentially bind the folded conformation of $GABA_A$ receptors. Therefore, Hsp47 promotes the subunit-subunit interaction, the receptor assembly process, and the anterograde trafficking of $GABA_A$ receptors. These Hsp47 properties are also extended to other Cys-loop receptors, including nicotinic acetylcholine receptors. Therefore, in addition to its known function as a collagen chaperone, this work establishes that Hsp47 also plays a critical and general role in the maturation of multi-subunit neuroreceptors.

INTRODUCTION

Initially, the term "molecular chaperone" was coined to describe a nuclear protein that enables the assembly of nucleosomes from folded histone proteins and DNA [1,2]. Since then, the role of chaperones, including the heat shock proteins, in facilitating protein folding [3,4] and maintaining protein homeostasis (proteostasis) at the cellular, tissue, and organismal levels has been extensively explored [5-7]. Proteostasis deficiencies have been recognized in a growing number of neurodegenerative, neurological, and metabolic diseases [8-10]. Strategies to restore proteostasis, including applying regulators of the unfolded protein response (UPR) and Ca^{2+} regulation, have been actively developed to ameliorate such protein conformational diseases [11-15]. However, despite recent progress, the role of chaperones in regulating the folding and assembly of multi-subunit membrane proteins requires further elucidation [16,17].

Multi-subunit membrane protein assembly in the endoplasmic reticulum (ER) is intimately linked to their folding and ER-associated degradation (ERAD). The current limited knowledge about the assembly process was gained from studying various classes of membrane proteins, including dimeric T cell receptors [18], trimeric P2X receptors [19], trimeric sodium channels [20], tetrameric potassium channels [21,22], and pentameric nicotinic acetylcholine receptors (nAChRs) [23,24]. We use γ-aminobutyric acid type A ($GABA_A$) receptors as a physiologically important substrate to study their biogenesis [25]. $GABA_A$ receptors are the primary inhibitory neurotransmitter-gated ion channels in mammalian central nervous systems [26] and provide most of the inhibitory tone to balance the tendency of excitatory neural circuits to induce hyperexcitability, thus maintaining the excitatory-inhibitory balance [27]. Functional $GABA_A$ receptors are assembled as pentamers in the ER from eight subunit classes: α1-6, β1-3, γ1-3, δ, ε, θ, π, and ρ1-3. The most common subtype in the human brain contains two α1

subunits, two β2 subunits, and one γ2 subunit [28]. To form a heteropentamer, individual subunits need to fold into their native structures in the ER [29,30] and assemble with other subunits correctly on the ER membrane [31,32] (**Figure S1**). Only properly assembled pentameric receptors exit the ER, traffic through the Golgi for complex glycosylation, and reach the plasma membrane to perform their function. It was demonstrated that the α1 subunits fail to exit the ER on their own and are retained in the ER; after their assembly with β subunits, the α1β complex can exit the ER for subsequent trafficking to the plasma membrane [32,33]. The inclusion of a γ2 subunit to form the pentamer further increases the conductance of the receptor and confers sensitivity to benzodiazepines [34]. Recently, it was reported that the synaptic localization of γ2-containing $GABA_A$ receptors requires the LHFPL family protein LHFPL4 and Neuroligin-2 [35]. However, many of the fundamental questions about how the proteostasis network regulates the multi-subunit membrane protein assembly process remains to be determined.

Elucidating the proteostasis network for the subunit folding and assembly process of multi-subunit membrane proteins and their biogenesis pathway in general, is important to fine-tune their function in physiological and pathological conditions. Loss of function of $GABA_A$ receptors is one prominent cause of genetic epilepsies [36,37]. Furthermore, numerous variations in a single subunit cause subunit protein misfolding in the ER and/or disrupt assembly of the pentameric complex, leading to excessive ERAD, decrease cell surface localization of the receptor complex, and result in imbalanced neural circuits [25,38]. The elucidation of the $GABA_A$ receptor proteostasis network will guide future efforts to develop strategies that restore

proteostasis of variant $GABA_A$ receptors to ameliorate corresponding diseases, such as genetic epilepsies.

Recently, our quantitative affinity purification mass spectrometry-based proteomics analysis identified Hsp47 (Gene: *SERPINH1*) as the most enriched $GABA_A$ receptor-interacting chaperone [39]. Hsp47 is an ER-resident protein with a RDEL (Arg-Asp-Glu-Leu) ER retention signal [40,41]. Among the large Serpin (*ser*ine *p*rotease *in*hibitor) superfamily, Hsp47 is the only one reported to show a molecular chaperone function [42]. Current literature describes Hsp47 as a collagen-specific chaperone [43,44]. However, its broader role has been indicated [45], such as interacting with the inositol-requiring enzyme 1α (IRE1α) to regulate the UPR [46] as well as interacting with amyloid precursor protein (APP) in the central nervous system (CNS) [47]. Here, we demonstrate that Hsp47 enhances the functional surface expression of both endogenous $GABA_A$ receptors, and other Cys-loop receptors in the CNS. Furthermore, a mechanistic study revealed that Hsp47 promotes the folding and assembly of multi-subunit neuroreceptors in the ER. Consequently, our results support a general role of Hsp47 in multi-subunit membrane protein quality control.

RESULTS

Hsp47 directly interacts with $GABA_A$ receptor subunits

Since we previously identified Hsp47 as the most enriched $GABA_A$ receptor-interacting chaperone in HEK293T cells using quantitative proteomics [39], here we evaluated the interaction between Hsp47 and $GABA_A$ receptors in more detail. Co-immunoprecipitation assays using mouse brain homogenates showed that the endogenous Hsp47 binds to endogenous $GABA_A$ receptor α1 subunits in the CNS (**Figure 1A**). Furthermore, to test a direct interaction

between Hsp47 and $GABA_A$ receptor subunits, we carried out an *in vitro* binding assay using recombinant GST-tagged α1 or β2 subunits and recombinant His-tagged Hsp47. The anti-His antibody pulldown detected the α1 subunit in the GST-α1 complex (**Figure 1B**, lane 5) and the β2 subunit in the GST-β2 complex (**Figure 1B**, lane 10). No α1 or β2 bands were detected in the GST control complex (**Figure 1B**, lanes 4 and 9), indicating that Hsp47 directly binds to the $GABA_A$ receptor α1 and β2 subunits *in vitro*.

Since Hsp47 resides in the ER lumen, it presumably interacts with the $GABA_A$ receptor ER luminal domain (ERD). According to a circular dichroism study, the α1 subunit ERD domain adopts a well-defined secondary structure [48]. Therefore, we determined the binding affinity between α1(ERD) and Hsp47. A MicroScale Thermophoresis (MST) assay reported a strong interaction (dissociation constant, Kd = 102 ± 10 nM) between α1(ERD) and Hsp47 (**Figure 1C**). In addition, due to the established role of Binding immunoglobulin Protein (BiP), a Hsp70 family chaperone in the ER lumen, in binding $GABA_A$ receptors [49], we measured the binding affinity between α1(ERD) and BiP, showing a Kd = 1906 ± 210 nM (**Figure 1C**). Therefore, Hsp47 binds more strongly to $GABA_A$ receptors compared to BiP, possibly because Hsp47 and BiP bind different $GABA_A$ receptor folding states (see below).

Hsp47 positively regulates the functional surface expression of endogenous $GABA_A$ receptors in neurons

To the best of our knowledge, functional regulation of $GABA_A$ receptor and other ion channels by Hsp47 in the CNS has not been previously reported. Hsp47 is widely distributed in the CNS, including the cortex, hippocampus, hypothalamus, cerebellum, and olfactory bulb

tested (**Figure S2A),** which is consistent with the report that Hsp47 is robustly detected in primary cortical and hippocampal neurons and brain slices [47]. Concomitantly, $GABA_A$ receptors are also distributed in these brain areas (**Figure S2A**) [28,50].

Because $GABA_A$ receptors must reach the plasma membrane to act as ligand-gated ion channels, we first performed an indirect immunofluorescence microscopy experiment to evaluate how Hsp47 regulates their endogenous surface expression levels in primary rat hippocampal neurons. The application of anti-$GABA_A$ receptor subunit antibodies that recognize their extracellular N-termini without a prior membrane permeabilization step enabled us to label only the cell surface expressed proteins. Transduction of lentivirus carrying Hsp47 siRNA led to substantial depletion of Hsp47 in neurons (**Figure S2B**), and knocking down Hsp47 significantly decreased the surface staining of the major subunits of $GABA_A$ receptors, including the α1 subunits and β2/β3 subunits (**Figure 2A**, cf. column 2 to column 1). This result indicated that Hsp47 positively regulates the surface protein levels of endogenous $GABA_A$ receptors. Furthermore, whole-cell patch-clamp electrophysiology recordings demonstrated that depleting Hsp47 significantly decreased the peak GABA-induced currents from 1660 ± 413 pA in the presence of scrambled siRNA to 886 ± 157 pA after the application of lentivirus carrying Hsp47 siRNA in hippocampal neurons (**Figure 2B**). Collectively, the experiments in **Figure 2** unambiguously reveal a novel role of Hsp47 as a positive regulator of the functional surface expression of endogenous $GABA_A$ receptors, an important neuroreceptor.

Hsp47 preferentially binds the folded conformation of $GABA_A$ receptor subunits and promotes their ER-to-Golgi trafficking

Since Hsp47 is an ER luminal chaperone, we hypothesized that to enhance the surface trafficking of $GABA_A$ receptors, Hsp47 promotes their protein folding in the ER and subsequent anterograde trafficking. We used an endoglycosidase H (Endo H) enzyme digestion assay to monitor the ER-to-Golgi trafficking of $GABA_A$ receptors, also as a surrogate to determine whether $GABA_A$ receptors are folded and assembled properly in the ER [49]. The Endo H enzyme selectively cleaves after asparaginyl-*N*-acetyl-D-glucosamine (GlcNAc) in the N-linked glycans in the ER, but it cannot remove this oligosaccharide chain after the high mannose form is enzymatically remodeled in the Golgi. Therefore, Endo H resistant subunit bands represent properly folded and assembled, post-ER subunit glycoforms, which traffic at least to the Golgi. Due to the heterogeneity of $GABA_A$ receptor subunits in neurons, we employed HEK293T cells to exogenously express the major subtype of $GABA_A$ receptors containing α1, β2, and γ2 subunits for the mechanistic study [51]. The Endo H digestion assay showed that Hsp47 overexpression increased the Endo H resistant band intensity (**Figure 3A**, cf. lane 4 to lane 2) and the ER to Golgi trafficking efficiency, represented by the ratio of the Endo H resistant α1 band / total α1 band (**Figure 3A**, cf. lane 4 to lane 2; quantification shown in the **Figure 3A** bottom panel). This result indicated that Hsp47 enhanced the folding and assembly of $GABA_A$ receptors in the ER and thus their ER-to-Golgi trafficking.

We next evaluated how Hsp47 coordinates the folding and assembly of $GABA_A$ receptors. We perturbed α1 subunit folding both genetically and chemically in HEK293T cells expressing $GABA_A$ receptors. We then evaluated the correlation between the relative folding degree of the α1 subunits and their interaction with Hsp47 using a co-immunoprecipitation assay. Individual $GABA_A$ receptor subunits have a signature disulfide bond in their large N-

terminal domain. Adding dithiothreitol (DTT), which is cell-permeable, to the cell culture media for 10 min destroyed the signature disulfide bond between Cys166 and Cys180 in the α1 subunit, thus compromising its folding. This operation did not change the total α1 protein levels (**Figure 3B**, cf. lanes 2-4 to lane 1) possibly because, during such a short time, degradation of the misfolded α1 subunit was not substantial. In sharp contrast, adding DTT significantly decreased the α1 protein that was pulled down by Hsp47 in a dose-dependent manner (**Figure 3B,** cf. lanes 7-9 to lane 6, quantification shown in the bottom panel). This indicates that eliminating the signature disulfide bond in the α1 subunit decreased its interaction with Hsp47 and supports the hypothesis that Hsp47 preferentially binds to the folded α1 subunit conformation.

In addition, we genetically disrupted the signature disulfide bond in the α1 subunit either by introducing a single C166A mutation or C166A/C180A double mutations. The co-immunoprecipitation assay clearly demonstrated that both the single and double mutations led to a decreased interaction between the α1 subunit and Hsp47 (**Figure 3C**, cf. lanes 6 and 7 to lane 5, quantification shown in the bottom panel). To evaluate the relative conformational stability of the α1 subunit variants, we examined the Triton X-100 detergent soluble fractions and the Triton X-100 detergent-insoluble fractions. The percentage of the insoluble fractions in the C166A single mutation and the C166A/C180A double mutations is significantly greater than that in the WT receptors (**Figure 3D**, quantification shown in the bottom panel), indicating that disrupting the signature disulfide bond induces aggregation. Notably, the C166A single mutant is more prone to aggregation than the C166A/C180A double mutant, which is not surprising because the single C166A mutant subunit retains an unpaired Cys180 in the ER lumen that remains available for cross-linking.

During the biogenesis in the ER, $GABA_A$ receptors need to interact with a network of chaperones and folding enzymes, such as BiP, to acquire their native structures [39]. BiP, which binds the hydrophobic patches of unfolded proteins and prevents their aggregation [52,53], interacts with the $GABA_A$ receptors in the ER [32,49]. We reasoned that if Hsp47 preferentially binds the folded conformation of the $GABA_A$ receptor subunits, it would act after BiP because BiP is expected to act early in the protein folding step in the ER [54,55]. We therefore evaluated how disrupting appropriate α1 subunit folding influenced their interaction with BiP. As hypothesized, the interactions between the α1 subunits and BiP were significantly enhanced when the signature disulfide bonds were chemically destroyed by adding DTT to the cell culture media (**Figure 3E,** cf. lanes 7, 8, and 9 to lane 6, quantification shown in the bottom panel). Genetic destruction of the α1 subunit disulfide bonds in the C166A single mutant or the C166A/C180A double mutant (**Figure 3F** cf. lanes 6 and 7 to lane 5, quantification shown in the bottom panel) produced similar results. Collectively, **Figure 3** indicates that inducing misfolding of $GABA_A$ receptors compromises their interactions with Hsp47, whereas, in sharp contrast, enhances their interactions with BiP. Therefore, BiP preferentially binds the unfolded/misfolded states, whereas Hsp47 preferentially binds the properly folded states of the α1 subunits. Hsp47 must therefore acts after BiP to enhance the productive folding of $GABA_A$ receptors.

Hsp47 enhances the subunit-subunit assembly of $GABA_A$ receptors

A cellular environment is required for the assembly of the majority of ion channels [23], indicating that factors other than ion channel subunits themselves are necessary in this process. We next tested our hypothesis that Hsp47 promotes efficient $GABA_A$ receptor subunit assembly. We used Förster resonance energy transfer (FRET) to evaluate the cellular interactions between

$GABA_A$ receptor subunits. We incorporated enhanced cyan fluorescent protein (CFP) (donor) into the TM3-TM4 intracellular loop of the α1 subunit and enhanced yellow fluorescent protein (YFP) (acceptor) into the TM3-TM4 intracellular loop of the β2 subunit. The addition of CFP/YFP into the large intracellular loops of $GABA_A$ receptors did not change the function of $GABA_A$ receptors since dose response to GABA was indistinguishable between α1β2γ2 receptors and (CFP-α1)(YFP-β2)γ2 receptors according to patch-clamp electrophysiology recordings in HEK293T cells (data not shown). The TM3-TM4 intracellular loops are the most variable segment within $GABA_A$ receptor subunits and their splice variants. These were often replaced with short sequences in structural studies [56,57]. Intracellular loops that incorporated CFP or YFP were also utilized in FRET experiments performed on nAChRs [58], members of the same Cys-loop superfamily to which $GABA_A$ receptors belong. Pixel-based FRET experiments showed that mean FRET efficiency was 24.4 ± 3.1% for (CFP-α1)(YFP-β2)γ2 receptors (**Figure 4A**, row 1, column 3); overexpressing Hsp47 significantly increased the mean FRET efficiency to 31.7 ± 5.7% (**Figure 4A**, row 2, column 3), indicating that Hsp47 positively regulates the assembly between α1 and β2 subunits of $GABA_A$ receptors. In addition, the co-immunoprecipitation assay showed that overexpression of Hsp47 significantly increased the relative amount of the β2 subunit that was pulled down with the α1 subunit (**Figure 4B**, cf. lane 5 to 4, quantification shown on the bottom), indicating that Hsp47 promotes incorporation of β2 subunits into $GABA_A$ receptor pentamers.

Further, we used non-reducing protein gels to evaluate how Hsp47 influences the formation of the oligomeric subunits during the assembly process in the ER. The absence of reducing reagents in the protein gel's sample loading buffer preserves the intra- and inter-subunit

disulfide bonds, which is expected to enable the detection of subunit oligomerization. In HEK293T cells expressing α1β2 receptors, distinct bands around 480 kDa were visible for both α1 subunit and β2 subunit in non-reducing gels (**Figure 4C**, lanes 2 to 5), indicating that the 480 kDa complex corresponds to the α1β2 hetero-oligomers. Moreover, the apparent molecular weight of the 480 kDa complex agrees with the molecular weight of the detected native $GABA_A$ receptors obtained from the cerebellum using blue native protein gels [35]. Therefore, the 480 kDa complex probably corresponds to the correctly assembled receptor complex. Strikingly, overexpression of Hsp47 increased the intensity of the 480 kDa bands for both α1 and β2 subunits (**Figure 4C**, cf. lanes 3-5 to lane 2, quantification in **Figure 4D**), indicating that Hsp47 promotes the formation of the properly assembled oligomers. In addition, reducing protein gels showed that overexpressing Hsp47 increased the band intensities for α1 and β2 subunits at 50 kDa in HEK293T cells expressing α1β2 receptors (**Figure 4C**, cf. lanes 8 to 10 to lane 7, quantification in **Figure 4E**). Moreover, we carried out control experiments using HEK293T cells expressing only α1 subunits because α1 subunits alone cannot exit the ER [33]. Non-reducing gels revealed that the majority of the detected α1 protein was in the monomeric form (**Figure 4C**, lane 12), and overexpression of Hsp47 did not change the intensity of α1 subunit band on the non-reducing gels (**Figure 4C**, cf. lanes 13-15 to lane 12) or using reducing gels (**Figure 4C**, cf. lanes 18-20 to lane 17). This probably occurred because α1 subunits alone cannot assemble to form a trafficking-competent complex to exit the ER. Collectively, these results indicated that Hsp47 promotes the assembly of the native pentameric $GABA_A$ receptor complexes for their subsequent ER exit and trafficking to the Golgi and plasma membrane.

Hsp47 rescues the function of epilepsy-associated $GABA_A$ receptors carrying the α1(A322D) variant

We next evaluated the effect of Hsp47 on the trafficking and function of pathogenic $GABA_A$ receptors using a well-characterized misfolding-prone α1(A322D) variant [59]. The A322D mutation introduces an extra negative charge in the TM3 helix of the α1 subunit, leading to inefficient insertion of TM3 into the lipid bilayer and fast degradation of the α1 subunit [49,59]. As a result, the α1(A322D) variant causes loss of function of $GABA_A$ receptors and juvenile myoclonic epilepsy [60]. An Endo H enzyme digestion assay showed that overexpressing Hsp47 increased the ratio of Endo H resistant α1 / total α1 bands from 0.20 ± 0.03 to 0.35 ± 0.08 (**Figure 5A**, cf. lane 4 to 2), indicating that Hsp47 promoted the formation of properly folded and assembled $GABA_A$ receptors in the ER and increased the trafficking efficiency of the α1(A322D) variant from the ER to the Golgi. Furthermore, surface biotinylation assays demonstrated that overexpressing Hsp47 significantly increased α1(A322D) variant surface expression (**Figure 5B**). The Hsp47-enhanced α1(A322D) surface expression was also reflected in the GABA-induced I_{max} from 8.5 ± 4.4 pA (n = 20) to 50.3 ± 19.7 pA (n = 17) in HEK293T cells expressing α1(A322D)β2γ2 $GABA_A$ receptors (**Figure 5C**). Therefore, Hsp47 promotes the functional surface expression of an epilepsy-associated $GABA_A$ receptor variant.

Hsp47 positively regulates the assembly and function of α4β2 nicotinic acetylcholine receptors (nAChRs)

The role of Hsp47 in regulating the maturation of ion channels has not been previously documented. We therefore expanded our investigation of the effect of Hsp47 to other members of the Cys-loop superfamily, to which $GABA_A$ receptors belong [61]. The Cys-loop receptors, including nAChRs, are pentameric ligand-gated neuroreceptors, sharing a common structural scaffold, including a β-sheet-rich ER lumen domain [62,63]. We chose to evaluate the effect of Hsp47 on heteropentameric α4β2 nAChRs and homopentameric α7 nAChRs since they are the major subtypes in the CNS [64]. Previously, FRET experiments were developed to evaluate the assembly of α4β2 and α7 nAChRs [58,65,66]. Here, FRET assays demonstrated that overexpressing Hsp47 significantly increased the mean FRET efficiency of (CFP-β2)(YFP-α4) nAChRs from 27.6% to 40.7% (**Figure 6A**), indicating that Hsp47 positively regulates the assembly of heteropentameric α4β2 receptors. In contrast, FRET experiments showed that Hsp47 overexpression did not influence the mean FRET efficiency of homopentameric α7 nAChRs (**Figure S3**), indicating that Hsp47 regulates the assembly of α4β2 and α7 nAChRs differently.

Furthermore, Hsp47 overexpression increased the nicotine-induced peak current from 57.9 ± 28.6 pA (n = 9) to 134 ± 84 pA (n = 9) in HEK293T cells expressing α4β2 nAChRs (**Figure 6B**). Therefore, Hsp47 positively regulates the assembly and thus function of α4β2 nAChRs. It appears that Hsp47 has a general role in promoting the maturation of multi-subunit neurotransmitter-gated ion channels.

DISCUSSION

Figure 7 illustrates our proposed mechanism for Hsp47 positively regulating the surface trafficking of $GABA_A$ receptors. BiP and calnexin assist the subunit folding early in the ER lumen [49]. Hsp47 operates after BiP and binds the folded states or late folding stage of the α1 and β2 subunits in the ER lumen. Hsp47 binding links the α1 and β2 subunits and enhances their inter-subunit interactions. As a result, Hsp47 promotes the formation of the assembly intermediates and the native pentameric receptors in the ER. The composition of the assembly intermediates, such as dimers and trimers, requires future investigation. Properly assembled receptors will traffic to the Golgi and onward to the plasma membrane for function. In addition, we demonstrated that Hsp47 positively regulates the assembly and function of α4β2 nAChRs, but not the assembly of α7 nAChRs. Interestingly, it was reported that RIC-3, an ER transmembrane protein, is important for the assembly of α7, but not α4β2 nAChRs [67,68], whereas NACHO (gene symbol: *TMEM35*), an ER transmembrane protein in the ER, can promote the assembly and function of both α4β2 and α7 nAChRs [24]. Therefore, the differential role of chaperones on the assembly of various subtypes of multi-subunit ion channels requires further investigation. Nonetheless, it appears that Hsp47 acts as a chaperone that promotes the assembly process of both $GABA_A$ receptors and α4β2 nAChRs from the Cys-loop receptor family. This supplements the canonical function of molecular chaperones that serve to assist protein folding and prevent protein aggregation. The assembly of $GABA_A$ receptor subunits is mediated by their N-terminal domains [51,69]. For example, residues 86-96 within α1 subunits, especially Gln95, play an important role in their assembly with β3 subunits [51]. Here, we showed that an ER lumen localized chaperone, Hsp47, enhanced the oligomerization of

hetero-pentameric $GABA_A$ receptors. It would be of great interest to identify the residues that mediate the interaction between Hsp47 and $GABA_A$ receptors.

Our results expand the client protein pool and function of Hsp47. Hsp47 was identified and is currently recognized as a collagen-specific chaperone [40]. Here, we demonstrate that Hsp47 has a general effect in proteostasis maintenance of both the $GABA_A$ receptor and nAChRs in the Cys-loop receptor superfamily. In addition, it was previously reported that Hsp47 physically interacts with amyloid precursor protein and regulates the secretion of Aβ-peptide [47]. Therefore, Hsp47 could have diverse functions in the CNS. Here, we show that Hsp47 binds the ER luminal domain (ERD) of $GABA_A$ receptor α1 subunit with high-affinity. The $GABA_A$ receptor ERD domain is rich in β-sheets containing ten β-strands [70], whereas, for its known substrate collagen, Hsp47 preferentially binds to the folded conformation of the collagen triple helices with a 2:1 stoichiometry [71-73]. It is also known that Hsp47 interacts with the ERD of IRE1α, a major transducer of the UPR, with a Kd of 73.2 ± 8.4 nM, to regulate the IRE1α oligomerization [46]; the ERD of IRE1α also adopts a β-sheet rich structure with a triangular assembly of β-sheet clusters [74]. Therefore, it appears that Hsp47 can interact with both the β-sheet-rich structure and triple helix structure. How Hsp47 adopts these structurally diverse client proteins will be the subject of future investigations. As a pentameric channel, each $GABA_A$ receptor has five potential binding sites for Hsp47. However, each $GABA_A$ receptor only has two agonist binding sites in the N-terminal domain for GABA. Therefore, the binding stoichiometry between Hsp47 and the pentameric $GABA_A$ receptors merits future effort.

Recent advances in genetics identified mutations in $GABA_A$ receptors that are associated with idiopathic epilepsies [36,38,75]. One mutation can compromise the receptor function by

influencing the protein biogenesis pathways (transcription, translation, folding, assembly, trafficking, and endocytosis), ligand binding, channel gating, or their combinations. Recently, we showed that enhancing the ER folding capacity is a viable way to restore the surface expression and thus function of misfolding-prone mutations [15,49,76-79]. Numerous disease-causing mutations disrupt their folding and/or assembly, leading to reduced trafficking to the plasma membrane. These trafficking-deficient mutant subunits are retained in the ER and degraded by the ERAD pathway. Because we envisage that Hsp47 stabilizes the assembled receptor complex, overexpressing Hsp47 has the promise to enhance the forward trafficking process of such mutant receptors, consequently restoring their normal function. Indeed, we show that Hsp47 partially restored the function of the misfolding-prone α1(A322D) subunit. This strategy serves as a proof-of-principle case for promoting the multi-subunit assembly process in order to ameliorate diseases resulting from membrane protein folding/assembly deficiencies.

MATERIALS AND METHODS

Plasmids

The pCMV6 plasmids containing human $GABA_A$ receptor α1 subunit (Uniprot #: P14867-1) (catalog #: RC205390), β2 subunit (isoform 2, Uniprot #: P47870-1) (catalog #: RC216424), γ2 subunit (isoform 2, Uniprot #: P18507-2) (catalog #: RC209260), and pCMV6 Entry Vector plasmid (pCMV6-EV) (catalog #: PS100001) were obtained from Origene. The missense mutations (A322D, C166A, or C166A/C180A in the $GABA_A$ receptor α1 subunit) were constructed using a QuikChange II site-directed mutagenesis Kit (Agilent Genomics, catalog #: 200523). A FLAG tag was inserted between Leu31 and Gln32 of the α1 subunit and between Asn28 and Asp29 of the β2 subunit of $GABA_A$ receptors by using QuikChange II site-directed mutagenesis. For $GABA_A$ receptors, enhanced cyan fluorescent protein (CFP) was inserted between Lys364 and Asn365 in the TM3-TM4 intracellular loop of the α1 subunit, and enhanced yellow fluorescent proteins (YFP) was inserted between Lys359 and Met360 in the TM3-TM4 intracellular loop of the β2 subunit by using the GenBuilder cloning kit (GenScript, catalog #: L00701). The construction of fluorescently tagged nAChR subunits were described previously [58,65]: CFP was inserted into the TM3-TM4 intracellular loop of the β2 subunit (Addgene, catalog #: 15106), YFP was inserted into TM3-TM4 intracellular loop of the α4 subunit (Addgene, catalog #: 15245), and cerulean (a CFP variant) or venus (a YFP variant) was inserted into TM3-TM4 intracellular loop of the α7 subunit. The human Hsp47 cDNA in pCMV6-XL5 plasmid was obtained from Origene (catalog#: SC119367). Scrambled siRNA GFP lentivector (catalog #: LV015-G) and Hsp47-set of four siRNA lentivectors (rat) (catalog #: 435050960395) were obtained from Applied Biological Materials. psPAX2 (Addgene plasmid #

12260; http://n2t.net/addgene:12260; RRID:Addgene_12260) and pMD2.G (Addgene plasmid # 12259; http://n2t.net/addgene:12259; RRID:Addgene_12259) were a gift from Didier Trono.

Antibodies

The mouse monoclonal anti-α1 subunit antibody (clone BD24, catalog #: MAB339), mouse monoclonal anti-β2/3 subunit antibody (clone 62-3G1, catalog #: 05-474), rabbit polyclonal anti-β2 subunit antibody (catalog #: AB5561), and rabbit polyclonal anti-NeuN (catalog #: ABN78) antibody were obtained from Millipore (Burlington, MA). The rabbit polyclonal anti-α1 antibody (catalog #: PPS022) was purchased from R&D systems (Minneapolis, MN), and the goat polyclonal anti-α1 subunit antibody (A-20; catalog #: SC-31405) was obtained from Santa Cruz Biotechnology (Dallas, TX). The mouse monoclonal anti-FLAG (catalog #: F1804) and anti-β-actin (catalog #: A1978) antibodies came from Sigma (St. Louis, MO). The mouse monoclonal anti-Hsp47 antibody (catalog #: ADI-SPA-470-F) came from Enzo Life Sciences (Farmingdale, NY). The rabbit polyclonal anti-Grp78 (BiP) antibody (catalog #: 3158-1) was obtained from Epitomics (Burlingame, CA). The rabbit polyclonal anti-Na^+/K^+ ATPase antibody (catalog #: AB76020) was obtained from Abcam (Waltham, MA). The mouse monoclonal anti-His tag antibody (catalog #: 2366S) was obtained from Cell Signaling Technology (Danvers, MA).

Cell Culture and Transfection

HEK293T cells (ATCC, catalog #: CRL-3216) were maintained in Dulbecco's Modified Eagle Medium (DMEM) (Fisher Scientific, Waltham, MA, catalog #: 10-013-CV) with 10% heat-inactivated fetal bovine serum (Fisher Scientific, catalog #: SH30396.03HI) and 1% Penicillin-Streptomycin (Fisher Scientific, catalog #: SV30010) at 37°C in 5% CO_2. Monolayers

were passaged upon reaching confluency with 0.05% trypsin protease (Fisher Scientific, catalog #: SH30236.01). Cells were grown in 6-well plates or 10 cm dishes and allowed to reach ~70% confluency before transient transfection using TransIT-2020 (Mirus Bio, Madison, WI, catalog #: MIR 5400) according to the manufacturer's instruction. HEK293T cells stably expressing α1β2γ2 or α1(A322D)β2γ2 $GABA_A$ receptors were generated using the G418 selectin method, as described previously [15,77]. Forty-eight hours post-transfection, cells were harvested for protein analysis.

Lentivirus transduction in rat neurons

Lentivirus production and transduction in neurons was performed as described previously [80]. Briefly, HEK293T cells were transfected with a Hsp47-set of four siRNA lentivectors (rat) (Applied Biological Materials, catalog #: 435050960395), or scrambled siRNA GFP lentivector (Applied Biological Materials, catalog #: LV015-G) together with psPAX2 and pMD2.G plasmids using TransIT-2020. The medium was changed after 8 h incubation, and cells were incubated for additional 36-48 h. Then the medium was collected, filtered, and concentrated using Lenti-X concentrator (Takara Bio, Catalog #: 631231). The lentivirus was quantified with the qPCR lentivirus titration kit (Applied Biological Materials, catalog #: LV900), and stored at −80°C.

Sprague Dawley rat E18 hippocampus was obtained from BrainBits (Springfield, IL). Neurons were isolated and cultured following the company's instruction. Briefly, tissues were digested with papain (2 mg/ml) (Sigma, catalog #: P4762) at 30°C for 10 min and triturated with a fire-polished sterile glass pipette for 1 min. Neurons were then plated onto poly-D-lysine (PDL) (Sigma, catalog #: P6407) and Laminin (Sigma, catalog #: L2020)-coated glass coverslips in a 24-well plate. Neurons were maintained in neuronal culture media containing Neurobasal

(ThermoFisher, catalog #: 21103049), 2% B27 (ThermoFisher, catalog #: 17504044), 0.5 mM GlutaMax (ThermoFisher, catalog #: 35050061), and 1% penicillin-streptomycin (Fisher Scientific, catalog #: SV30010) at 37°C in 5% CO_2. Neurons were subjected to transduction with lentivirus at days *in vitro* (DIV) 10, and immunofluorescence staining and electrophysiology were performed at DIV 12.

Mouse brain homogenization

C57BL/6J mice (Jackson Laboratory) at 8-10 weeks were sacrificed and the cortex was isolated and homogenized in the homogenization buffer (25 mM Tris, pH 7.6, 150 mM NaCl, 1 mM EDTA, and 2% Triton X-100) supplemented with the Roche complete protease inhibitor cocktail (Roche; catalog #: 4693159001). The homogenates were centrifuged at 800 × g for 10 min at 4 °C, and the supernatants were collected. The pellet was re-homogenized in additional homogenization buffer and centrifuged at 800 × g for 10 min at 4 °C. The supernatants were combined and rotated for 2 h at 4 °C, and then centrifuged at 15,000 × g for 30 min at 4 °C. The resulting supernatant was collected as mouse brain homogenate. Protein concentration was determined by a MicroBCA assay (Pierce, catalog #: 23235). This animal study was approved by the Institutional Animal Care and Use Committees (IACUC) at Case Western Reserve University and was carried out in agreement with the recommendation of the American Veterinary Medical Association Panel on Euthanasia.

Western Blot Analysis

Cells were harvested and lysed with lysis buffer (50 mM Tris, pH 7.5, 150 mM NaCl, and 1% Triton X-100) or RIPA buffer (50 mM Tris, pH 7.4, 150 mM NaCl, 5 mM EDTA, pH 8.0, 2% NP-40, 0.5% sodium deoxycholate, and 0.1% SDS) supplemented with Roche complete protease inhibitor cocktail. Lysates were cleared by centrifugation (20,000 × *g*, 10 min, 4 °C).

Protein concentration was determined by MicroBCA assay. Aliquots of cell lysates were separated in an 8% SDS-PAGE gel, and Western blot analysis was performed using the appropriate antibodies. Band intensity was quantified using ImageJ software from the National Institute of Health [81]. For non-reducing protein gels, cell lysates were loaded in the Laemmli sample buffer (Biorad, Hercules, CA, catalog #: 1610737); for reducing protein gels, cell lysates were loaded in the Laemmli sample buffer (Biorad, catalog #: 1610737) supplemented with 100 mM dithiothreitol (DTT) to reduce the disulfide bonds. Endoglycosidase H (endo H) (New England Biolabs, catalog #: P0703L) enzyme digestion or Peptide-N-Glycosidase F (PNGase F) (New England Biolabs, Ipswich, MA, catalog #: P0704L) enzyme digestion was performed according to manufacturer's instruction and the published procedure [49].

Immunoprecipitation

Cell lysates (500 μg) or mouse brain homogenates (1 mg) were pre-cleared with 30 μL of protein A/G plus-agarose beads (Santa Cruz Biotechnology, catalog #: SC-2003) and 1.0 μg of normal mouse IgG (Santa Cruz Biotechnology, catalog #: SC-2025) for 1 hour at 4°C to remove nonspecific binding proteins. The pre-cleared samples were incubated with 2.0 μg of mouse anti-α1 antibody, mouse anti-Hsp47 antibody, or normal mouse IgG as a negative control for 1 hour at 4°C and then with 30 μL of protein A/G plus agarose beads overnight at 4°C. Afterward, the beads were collected by centrifugation at 8000 ×g for 30 s, and washed three times with lysis buffer. The complex was eluted by incubation with 30 μL of Laemmli sample buffer loading buffer in the presence of 100 mM DTT. The immunopurified eluents were separated in an 8% SDS-PAGE gel, and Western blot analysis was performed using appropriate antibodies.

***In vitro* protein binding assay**

1 μg of GST epitope tag protein (GST) (Novus Biologicals, Centennial, CO, catalog #: NBC1-18537), GST-tagged human $GABA_A$ receptor α1 subunit protein (GST-α1) (Abnova, Walnut, CA, catalog #: H00002554-P01), or GST-tagged human $GABA_A$ receptor β2 subunit protein (GST-β2) (Abnova, catalog #: H00002561-P01) was mixed with 4 μg of recombinant His-tagged human Hsp47 protein (Novus, catalog #: NBC1-22576) in 500 μL of lysis buffer (50 mM Tris, pH 7.5, 150 mM NaCl, and 1% Triton X-100). The protein complex was isolated by immunoprecipitation using a mouse anti-His antibody (Cell Signaling, catalog #: 2366S) followed by SDS-PAGE and Western blot analysis with a rabbit anti-$GABA_A$ receptor α1 subunit antibody (R&D Systems, catalog #: PS022), a mouse anti-$GABA_A$ receptor β2/β3 subunit antibody (Millipore, catalog #: 05-474), or a mouse anti-His antibody.

MicroScale Thermophoresis (MST)

MST experiments were carried out to measure the binding affinity between the ER luminal domain of human $GABA_A$ receptor α1 subunits (α1-ERD) and ER luminal chaperones, Hsp47 and BiP, using a Monolith NT.115 instrument (NanoTemper Technologies Inc, South San Francisco, CA). Monolith His-Tag Labeling Kit RED-tris-NTA 2nd Generation (NanoTemper Technologies, catalog #: MO-L018) was used to label recombinant His-α1-ERD (MyBioSource, San Diego. CA, catalog #: MBS948971). 100 μL of 200 nM RED-tris-NTA dye in PBST buffer (137 mM NaCl, 2.7 mM KCl, 10 mM Na_2HPO_4, 1.8 mM KH_2PO_4, pH 7.4, 0.05% Tween-20) was mixed with 100 μL of 200 nM His-α1-ERD in PBST, and the reaction mixture was incubated for 30 min at room temperature in the dark. The serial dilutions of the ligand proteins (0.2 nM to 10 μM) in PBST, including recombinant human Hsp47 (Abcam, catalog #: ab86918) and human BiP (Abcam, catalog #: ab78432), were prepared in Maxymum Recovery PCR tubes

(Axygen, Union City, CA, catalog #: PCR-02-L-C) with a final volume of 5 μL in each tube. Then 5 μL of 100 nM RED labeled His-α1-ERD was added to each PCR tube containing 5 μL of the ligand proteins. The samples were loaded to the capillaries (NanoTemper Technologies, catalog #: MO-K025) and measured using a Monolith NT.115 instrument with the settings of 40% LED/excitation and 40% MST power. The data were collected and analyzed using the Monolith software for the calculation of the dissociation constant (Kd).

Biotinylation of Cell Surface Proteins

Cells were plated in 6-cm dishes for surface biotinylation experiments according to the published procedure [49]. Briefly, intact cells were washed twice with ice-cold Dulbecco's phosphate buffered saline (DPBS) (Fisher Scientific, catalog #: SH3002803). To label surface membrane proteins, cells were incubated with the membrane-impermeable biotinylation reagent Sulfo-NHS SS-Biotin (0.5 mg / mL) (Pierce, catalog #: 21331) in DPBS containing 0.1 mM $CaCl_2$ and 1 mM $MgCl_2$ (DPBS+CM) for 30 min at 4 °C. To quench the reaction, cells were incubated with 10 mM glycine in ice-cold DPBS+CM twice for 5 min at 4 °C. Sulfhydryl groups were blocked by incubating the cells with 5 nM N-ethylmaleimide (NEM) (Pierce, catalog #: 23030) in DPBS for 15 min at room temperature. Cells were then solubilized for 1 h at 4 °C in solubilization buffer (50 mM Tris–HCl, 150 mM NaCl, 5 mM EDTA, pH 7.5, 1% Triton X-100) supplemented with Roche complete protease inhibitor cocktail and 5 mM NEM. The samples were centrifuged at 20,000 × g for 10 min at 4 °C to pellet cellular debris. The supernatant contained the biotinylated surface proteins. The concentration of the supernatant was measured using microBCA assay. Biotinylated surface proteins were affinity-purified from the above supernatant by incubating for 1 h at 4 °C with 100 μL of immobilized neutravidin-conjugated agarose bead slurry (Pierce, catalog #: 29200). The samples were then centrifuged at 20,000 ×g

for 10 min at 4 °C. The beads were washed six times with solubilization buffer. Surface proteins were eluted from beads by boiling for 5 min with 200 μL of LSB / Urea buffer (2x Laemmli sample buffer (LSB) with 100 mM DTT and 6 M urea; pH 6.8) for SDS-PAGE and Western blotting analysis.

Immunofluorescence Staining and Confocal Microscopy

Neuron staining and confocal immunofluorescence microscopy analysis were performed as described previously [49,80]. Briefly, to label cell surface proteins, primary neurons on coverslips were fixed with 2% paraformaldehyde in DPBS for 10 min. We then blocked with 10% goat serum (ThermoFisher, catalog #: 16210064) in DPBS for 0.5 h, and without detergent permeabilization, incubated with 100 μL of appropriate primary antibodies against the $GABA_A$ receptor α1 subunit (Synaptic Systems, Goettingen, Germany, catalog #: 224203) (1:250 dilution) or β2/3 subunits (Millipore, catalog #: 05-474) (1:250 dilution), diluted in 2% goat serum in DPBS, at room temperature for 1 h. Then the neurons were incubated with Alexa 594-conjugated goat anti-rabbit antibody (ThermoFisher, catalog #: A11037), or Alexa 594-conjugated goat anti-mouse antibody (ThermoFisher, catalog #: A11032) (1:500 dilution) diluted in 2% goat serum in DPBS for 1 h. Afterward, cells were permeabilized with saponin (0.2%) for 5 min and incubated with DAPI (1 μg/mL) (ThermoFisher, catalog #: D1306) for 3 min to stain the nucleus. To label intracellular proteins, neurons were fixed with 4% paraformaldehyde in DPBS for 15 min, permeabilized with saponin (0.2%) in DPBS for 15 min, and blocked with 10% goat serum in DPBS for 0.5 h at room temperature. Then neurons were labeled with appropriate primary antibodies against Hsp47 (Enzo Life Sciences, catalog #: ADI-SPA-470-F) (1:100 dilution) or NeuN, a neuron nuclei marker (Millipore, catalog #: ABN78) (1:500 dilution), diluted in 2% goat serum in DPBS, for 1 h. The neurons were then incubated with

Alexa 594-conjugated goat anti-mouse antibody (ThermoFisher, catalog #: A11032) (1:500 dilution), or Alexa 350-conjugated goat anti-rabbit antibody (ThermoFisher, catalog #: A21068) (1:500 dilution), diluted in 2% goat serum in DPBS, for 1 h. The coverslips were then mounted using fluoromount-G (VWR, catalog #: 100502-406) and sealed. An Olympus IX-81 Fluoview FV1000 confocal laser scanning system was used for imaging with a 60× objective by using FV10-ASW software. The images were analyzed using ImageJ software [81].

Pixel-based sensitized acceptor emission FRET microscopy

Pixel-by-pixel based sensitized acceptor FRET microscopy was performed as described previously[65,82]. For FRET experiments on $GABA_A$ receptors, (1) for FRET pair samples, HEK293T cells on coverslips were transfected with α1-CFP (donor) (0.5 μg), β2-YFP (acceptor) (0.5 μg), and γ2 (0.5 μg) subunits; (2) for the donor-only samples, to determine the spectral bleed-through (SBT) parameter for the donor, HEK293T cells were transfected with α1-CFP (donor) (0.5 μg), β2 (0.5 μg), and γ2 (0.5 μg) subunits; (3) for the acceptor-only samples, to determine the SBT parameter for the acceptor, HEK293T cells were transfected with α1 (0.5 μg), β2-YFP (acceptor) (0.5 μg), and γ2 (0.5 μg) subunits. For FRET experiments on nAChRs, HEK293T cells were transfected with β2-CFP (donor) (0.7 μg) and α4-YFP (acceptor) (0.7 μg) or α7-cerulean (donor) (0.7 μg) and α7-venus (acceptor) (0.7 μg); in addition, the donor-only samples or the acceptor-only samples were prepared to determine the SBT parameters for the donor or the acceptor, respectively. Whole-cell patch-clamp recordings in HEK293T cells showed that fluorescently tagged ion channels have similar peak current amplitudes and dose-response curves to the agonists as compared to untagged ion channels [65]. The coverslips were then mounted using fluoromount-G and sealed. An Olympus Fluoview FV1000 confocal laser

scanning system was used for imaging with a 60× objective by using Olympus FV10-ASW software.

For the FRET pair samples, donor images were acquired at an excitation wavelength of 433 nm and an emission wavelength of 478 nm, FRET images at 433 nm excitation and 528 nm emission wavelengths, and acceptor images at 514 nm excitation and 528 nm emission wavelengths. For the donor-only samples, donor images were acquired at 433 nm excitation and 478 nm emission wavelengths, and FRET images at 433 nm excitation and 528 nm emission wavelengths. For the acceptor-only samples, FRET images were acquired at an excitation of 433 nm and an emission of 528 nm, and acceptor images at an excitation of 514 nm and an emission of 528 nm. Image analysis of FRET efficiencies was performed using the PixFRET plugin of the ImageJ software [83]. The bleed-through was determined for the donor and the acceptor. With the background and bleed-through correction, the net FRET (nFRET) was calculated according to equation (1).

$$nFRET = I_{FRET} - SBT_{donor} * I_{donor} - SBT_{acceptor} * I_{acceptor} \quad (1)$$

FRET efficiencies from sensitized emission experiments were calculated according to equation (2).

$$E_{FRET} = 1 - I_{DA} / I_{D} \quad (2)$$

EFRET represents FRET efficiency, IDA represents the emission intensity of the donor in the presence of the acceptor, and ID represents the emission intensity of the donor alone. Since ID can be estimated by adding the nFRET signal amplitude to the amplitude of IDA [84], FRET efficiency was calculated according to equation (3).

$$E_{FRET} = 1 - (I_{DA}/(I_{DA} + nFRET)) \quad (3)$$

Whole-Cell Patch-Clamp Electrophysiology

Whole-cell patch-clamp recording was performed at room temperature, as described previously for $GABA_A$ receptors [78] or nAChRs [85]. Briefly, the glass electrodes have a tip resistance of 3–5 MΩ when filled with intracellular solution. For $GABA_A$ receptor recording, the intracellular solution was composed of (in mM): 153 KCl, 1 $MgCl_2$, 5 EGTA, 10 HEPES, and 5 Mg-ATP (adjusted to pH 7.3 with KOH); the extracellular solution was composed of (in mM): 142 NaCl, 8 KCl, 6 $MgCl_2$, 1 $CaCl_2$, 10 glucose, 10 HEPES, and 120 nM fenvalerate (adjusted to pH 7.4 with NaOH). For nAChR recording, the intracellular solution was composed of (in mM): 135 K-gluconate, 5 KCl, 5 EGTA, 0.5 $CaCl_2$, 10 HEPES, 2 Mg-ATP, and 0.1 GTP (adjusted to pH 7.2 with Tris-base); the extracellular solution was composed of (in mM): 140 NaCl, 5 KCl, 2 $CaCl_2$, 1 $MgCl_2$, 10 HEPES, and 10 glucose (adjusted to pH 7.3 with Tris-base). For $GABA_A$ receptor recordings, coverslips containing cells were placed in a RC-25 recording chamber (Warner Instruments) on the stage of an Olympus IX-71 inverted fluorescence microscope and perfused with extracellular solution. Fast chemical application was accomplished with a pressure-controlled perfusion system (Warner Instruments) positioned within 50 µm of the cell utilizing a Quartz MicroManifold with 100-µm inner diameter inlet tubes (ALA Scientific). The whole-cell currents were recorded at a holding potential of −60 mV in voltage-clamp mode using an Axopatch 200B amplifier (Molecular Devices, San Jose, CA). The signals were acquired at 10 kHz and filtered at 2 kHz using pClamp10 software (Molecular Devices). For nAChR recordings, cells were visualized with an upright microscope (Axio Examiner A1, Zeiss) equipped with an Axiocam 702 mono camera. Whole-cell currents were recorded at a holding potential of -60 mV in voltage clamp mode using an Integrated Patch-Clamp Amplifier (Sutter). Signals were detected at 10 kHz and filtered at 2 kHz using SutterPatch acquisition software.

QUANTIFICATION AND STATISTICAL ANALYSIS

All data are presented as mean ± SD. If two groups were compared, statistical significance was calculated using an unpaired Student's t-test; if more than two groups were compared, we used ANOVA followed by post hoc Tukey. A $p < 0.05$ was considered statistically significant. *, $p < 0.05$; **, $p < 0.01$; ***, $p < 0.001$.

SUPPLEMENTAL INFORMATION

Supplemental Information includes three figures.

ACKNOWLEDGMENTS

This work was supported by the National Institutes of Health (R01NS105789 and R01NS117176 to TM). We thank Dr. Matthias Buck (Case Western Reserve University, Cleveland, Ohio) for the help from his group on the MST experiments.

AUTHOR CONTRIBUTIONS

Conceptualization, YW and TM; Data curation: YW, XD, DH, RN, BH, and FM; Formal analysis: YW, XD, DH, RN, BH, FM, and TM; Funding acquisition: TM; Supervision: TM; Writing – original draft: YW, XD, and TM; Writing – review & editing: YW, XD, RN, BH, FM, and TM.

DECLARATION OF INTERESTS

The authors declare no competing interests.

REFERENCES

1. ELLIS RJ (2013) ASSEMBLY CHAPERONES: A PERSPECTIVE. PHILOS TRANS R SOC LOND B BIOL SCI 368: 20110398.
2. LASKEY RA, HONDA BM, MILLS AD, FINCH JT (1978) NUCLEOSOMES ARE ASSEMBLED BY AN ACIDIC PROTEIN WHICH BINDS HISTONES AND TRANSFERS THEM TO DNA. NATURE 275: 416-420.
3. HARTL FU, BRACHER A, HAYER-HARTL M (2011) MOLECULAR CHAPERONES IN PROTEIN FOLDING AND PROTEOSTASIS. NATURE 475: 324-332.
4. HORWICH AL (2014) MOLECULAR CHAPERONES IN CELLULAR PROTEIN FOLDING: THE BIRTH OF A FIELD. CELL 157: 285-288.
5. BALCH WE, MORIMOTO RI, DILLIN A, KELLY JW (2008) ADAPTING PROTEOSTASIS FOR DISEASE INTERVENTION. SCIENCE 319: 916-919.
6. BALCHIN D, HAYER-HARTL M, HARTL FU (2016) IN VIVO ASPECTS OF PROTEIN FOLDING AND QUALITY CONTROL. SCIENCE 353: AAC4354.
7. SALA AJ, BOTT LC, MORIMOTO RI (2017) SHAPING PROTEOSTASIS AT THE CELLULAR, TISSUE, AND ORGANISMAL LEVEL. J CELL BIOL 216: 1231-1241.
8. FERRO-NOVICK S, REGGIORI F, BRODSKY JL (2021) ER-PHAGY, ER HOMEOSTASIS, AND ER QUALITY CONTROL: IMPLICATIONS FOR DISEASE. TRENDS BIOCHEM SCI 46: 630-639.
9. KELLY JW (2020) PHARMACOLOGIC APPROACHES FOR ADAPTING PROTEOSTASIS IN THE SECRETORY PATHWAY TO AMELIORATE PROTEIN CONFORMATIONAL DISEASES. COLD SPRING HARB PERSPECT BIOL 12.
10. WANG M, KAUFMAN RJ (2016) PROTEIN MISFOLDING IN THE ENDOPLASMIC RETICULUM AS A CONDUIT TO HUMAN DISEASE. NATURE 529: 326-335.
11. DAS I, KRZYZOSIAK A, SCHNEIDER K, WRABETZ L, D'ANTONIO M, ET AL. (2015) PREVENTING PROTEOSTASIS DISEASES BY SELECTIVE INHIBITION OF A PHOSPHATASE REGULATORY SUBUNIT. SCIENCE 348: 239-242.
12. GRANDJEAN JMD, WISEMAN RL (2020) SMALL MOLECULE STRATEGIES TO HARNESS THE UNFOLDED PROTEIN RESPONSE: WHERE DO WE GO FROM HERE? J BIOL CHEM 295: 15692-15711.
13. MU T-W, FOWLER DM, KELLY JW (2008) PARTIAL RESTORATION OF MUTANT ENZYME HOMEOSTASIS IN THREE DISTINCT LYSOSOMAL STORAGE DISEASE CELL LINES BY ALTERING CALCIUM HOMEOSTASIS. PLOS BIOLOGY 6: E26.
14. TUFANLI O, TELKOPARAN AKILLILAR P, ACOSTA-ALVEAR D, KOCATURK B, ONAT UI, ET AL. (2017) TARGETING IRE1 WITH SMALL MOLECULES COUNTERACTS PROGRESSION OF ATHEROSCLEROSIS. PROC NATL ACAD SCI U S A 114: E1395-E1404.
15. WANG M, COTTER E, WANG YJ, FU X, WHITTSETTE AL, ET AL. (2022) PHARMACOLOGICAL ACTIVATION OF ATF6 REMODELS THE PROTEOSTASIS NETWORK TO RESCUE PATHOGENIC GABA(A) RECEPTORS. CELL BIOSCI 12: 48.
16. HEGDE RS (2022) THE FUNCTION, STRUCTURE, AND ORIGINS OF THE ER MEMBRANE PROTEIN COMPLEX. ANNU REV BIOCHEM.

17. MCKENNA MJ, SIM SI, ORDUREAU A, WEI L, HARPER JW, ET AL. (2020) THE ENDOPLASMIC RETICULUM P5A-ATPASE IS A TRANSMEMBRANE HELIX DISLOCASE. SCIENCE 369.
18. FEIGE MJ, BEHNKE J, MITTAG T, HENDERSHOT LM (2015) DIMERIZATION-DEPENDENT FOLDING UNDERLIES ASSEMBLY CONTROL OF THE CLONOTYPIC ALPHABETAT CELL RECEPTOR CHAINS. J BIOL CHEM 290: 26821-26831.
19. BOUMECHACHE M, MASIN M, EDWARDSON JM, GORECKI DC, MURRELL-LAGNADO R (2009) ANALYSIS OF ASSEMBLY AND TRAFFICKING OF NATIVE P2X4 AND P2X7 RECEPTOR COMPLEXES IN RODENT IMMUNE CELLS. J BIOL CHEM 284: 13446-13454.
20. BUCK TM, JORDAHL AS, YATES ME, PRESTON GM, COOK E, ET AL. (2017) INTERACTIONS BETWEEN INTERSUBUNIT TRANSMEMBRANE DOMAINS REGULATE THE CHAPERONE-DEPENDENT DEGRADATION OF AN OLIGOMERIC MEMBRANE PROTEIN. BIOCHEM J 474: 357-376.
21. DELANEY E, KHANNA P, TU L, ROBINSON JM, DEUTSCH C (2014) DETERMINANTS OF PORE FOLDING IN POTASSIUM CHANNEL BIOGENESIS. PROC NATL ACAD SCI U S A 111: 4620-4625.
22. LI K, JIANG Q, BAI X, YANG YF, RUAN MY, ET AL. (2017) TETRAMERIC ASSEMBLY OF K+ CHANNELS REQUIRES ER-LOCATED CHAPERONE PROTEINS. MOL CELL 65: 52-65.
23. GREEN WN (1999) PERSPECTIVE - ION CHANNEL ASSEMBLY: CREATING STRUCTURES THAT FUNCTION. JOURNAL OF GENERAL PHYSIOLOGY 113: 163-169.
24. GU S, MATTA JA, LORD B, HARRINGTON AW, SUTTON SW, ET AL. (2016) BRAIN ALPHA7 NICOTINIC ACETYLCHOLINE RECEPTOR ASSEMBLY REQUIRES NACHO. NEURON 89: 948-955.
25. FU YL, WANG YJ, MU TW (2016) PROTEOSTASIS MAINTENANCE OF CYS-LOOP RECEPTORS. ADV PROTEIN CHEM STRUCT BIOL 103: 1-23.
26. MACDONALD RL, OLSEN RW (1994) GABA(A) RECEPTOR CHANNELS. ANNUAL REVIEW OF NEUROSCIENCE 17: 569-602.
27. KIRMSE K, ZHANG C (2022) PRINCIPLES OF GABAERGIC SIGNALING IN DEVELOPING CORTICAL NETWORK DYNAMICS. CELL REP 38: 110568.
28. SEQUEIRA A, SHEN K, GOTTLIEB A, LIMON A (2019) HUMAN BRAIN TRANSCRIPTOME ANALYSIS FINDS REGION- AND SUBJECT-SPECIFIC EXPRESSION SIGNATURES OF GABA(A)R SUBUNITS. COMMUN BIOL 2: 153.
29. ALDER NN, JOHNSON AE (2004) COTRANSLATIONAL MEMBRANE PROTEIN BIOGENESIS AT THE ENDOPLASMIC RETICULUM. J BIOL CHEM 279: 22787-22790.
30. SKACH WR (2009) CELLULAR MECHANISMS OF MEMBRANE PROTEIN FOLDING. NATURE STRUCTURAL & MOLECULAR BIOLOGY 16: 606-612.
31. BARNES EM (2001) ASSEMBLY AND INTRACELLULAR TRAFFICKING OF GABA(A) RECEPTORS. INTERNATIONAL REVIEW OF NEUROBIOLOGY, VOL 48. PP. 1-29.

32. CONNOLLY CN, KRISHEK BJ, MCDONALD BJ, SMART TG, MOSS SJ (1996) ASSEMBLY AND CELL SURFACE EXPRESSION OF HETEROMERIC AND HOMOMERIC GAMMA-AMINOBUTYRIC ACID TYPE A RECEPTORS. J BIOL CHEM 271: 89-96.
33. CONNOLLY CN, WOOLTORTON JR, SMART TG, MOSS SJ (1996) SUBCELLULAR LOCALIZATION OF GAMMA-AMINOBUTYRIC ACID TYPE A RECEPTORS IS DETERMINED BY RECEPTOR BETA SUBUNITS. PROC NATL ACAD SCI U S A 93: 9899-9904.
34. OLSEN RW, SIEGHART W (2009) GABA A RECEPTORS: SUBTYPES PROVIDE DIVERSITY OF FUNCTION AND PHARMACOLOGY. NEUROPHARMACOLOGY 56: 141-148.
35. YAMASAKI T, HOYOS-RAMIREZ E, MARTENSON JS, MORIMOTO-TOMITA M, TOMITA S (2017) GARLH FAMILY PROTEINS STABILIZE GABAA RECEPTORS AT SYNAPSES. NEURON 93: 1138-1152 E1136.
36. HERNANDEZ CC, MACDONALD RL (2019) A STRUCTURAL LOOK AT GABA(A) RECEPTOR MUTATIONS LINKED TO EPILEPSY SYNDROMES. BRAIN RES 1714: 234-247.
37. HIROSE S (2014) MUTANT GABA(A) RECEPTOR SUBUNITS IN GENETIC (IDIOPATHIC) EPILEPSY. PROG BRAIN RES 213: 55-85.
38. FU X, WANG YJ, KANG JQ, MU TW (2022) GABAA RECEPTOR VARIANTS IN EPILEPSY; CZUCZWAR SJ, EDITOR: BRISBANE (AU): EXON PUBLICATIONS.
39. WANG YJ, DI XJ, MU TW (2022) QUANTITATIVE INTERACTOME PROTEOMICS IDENTIFIES A PROTEOSTASIS NETWORK FOR GABA(A) RECEPTORS. J BIOL CHEM: 102423.
40. NAGATA K, SAGA S, YAMADA KM (1986) A MAJOR COLLAGEN-BINDING PROTEIN OF CHICK EMBRYO FIBROBLASTS IS A NOVEL HEAT SHOCK PROTEIN. J CELL BIOL 103: 223-229.
41. SAGA S, NAGATA K, CHEN WT, YAMADA KM (1987) PH-DEPENDENT FUNCTION, PURIFICATION, AND INTRACELLULAR LOCATION OF A MAJOR COLLAGEN-BINDING GLYCOPROTEIN. J CELL BIOL 105: 517-527.
42. DAFFORN TR, DELLA M, MILLER AD (2001) THE MOLECULAR INTERACTIONS OF HEAT SHOCK PROTEIN 47 (HSP47) AND THEIR IMPLICATIONS FOR COLLAGEN BIOSYNTHESIS. J BIOL CHEM 276: 49310-49319.
43. NAGATA K (2003) HSP47 AS A COLLAGEN-SPECIFIC MOLECULAR CHAPERONE: FUNCTION AND EXPRESSION IN NORMAL MOUSE DEVELOPMENT. SEMINARS IN CELL & DEVELOPMENTAL BIOLOGY 14: 275-282.
44. TAGUCHI T, RAZZAQUE MS (2007) THE COLLAGEN-SPECIFIC MOLECULAR CHAPERONE HSP47: IS THERE A ROLE IN FIBROSIS? TRENDS IN MOLECULAR MEDICINE 13: 45-53.
45. ITO S, NAGATA K (2019) ROLES OF THE ENDOPLASMIC RETICULUM-RESIDENT, COLLAGEN-SPECIFIC MOLECULAR CHAPERONE HSP47 IN VERTEBRATE CELLS AND HUMAN DISEASE. J BIOL CHEM 294: 2133-2141.
46. SEPULVEDA D, ROJAS-RIVERA D, RODRÍGUEZ DA, GROENENDYK J, KÖHLER A, ET AL. (2018) INTERACTOME SCREENING IDENTIFIES THE ER LUMINAL

CHAPERONE HSP47 AS A REGULATOR OF THE UNFOLDED PROTEIN RESPONSE TRANSDUCER IRE1A. MOL CELL 69: 238-252 E237.
47. BIANCHI FT, CAMERA P, ALA U, IMPERIALE D, MIGHELI A, ET AL. (2011) THE COLLAGEN CHAPERONE HSP47 IS A NEW INTERACTOR OF APP THAT AFFECTS THE LEVELS OF EXTRACELLULAR BETA-AMYLOID PEPTIDES. PLOS ONE 6: E22370.
48. SHI H, TSANG SY, TSE MK, XU Z, XUE H (2003) RECOMBINANT EXTRACELLULAR DOMAIN OF THE THREE MAJOR SUBUNITS OF GABAA RECEPTOR SHOW COMPARABLE SECONDARY STRUCTURE AND BENZODIAZEPINE BINDING PROPERTIES. PROTEIN SCI 12: 2642-2646.
49. DI XJ, HAN DY, WANG YJ, CHANCE MR, MU TW (2013) SAHA ENHANCES PROTEOSTASIS OF EPILEPSY-ASSOCIATED ALPHA1(A322D)BETA2GAMMA2 GABA(A) RECEPTORS. CHEM BIOL 20: 1456-1468.
50. RICHARDS JG, SCHOCH P, HARING P, TAKACS B, MOHLER H (1987) RESOLVING GABAA/BENZODIAZEPINE RECEPTORS: CELLULAR AND SUBCELLULAR LOCALIZATION IN THE CNS WITH MONOCLONAL ANTIBODIES. J NEUROSCI 7: 1866-1886.
51. TAYLOR PM, CONNOLLY CN, KITTLER JT, GORRIE GH, HOSIE A, ET AL. (2000) IDENTIFICATION OF RESIDUES WITHIN GABA(A) RECEPTOR ALPHA SUBUNITS THAT MEDIATE SPECIFIC ASSEMBLY WITH RECEPTOR BETA SUBUNITS. J NEUROSCI 20: 1297-1306.
52. FLYNN GC, POHL J, FLOCCO MT, ROTHMAN JE (1991) PEPTIDE-BINDING SPECIFICITY OF THE MOLECULAR CHAPERONE BIP. NATURE 353: 726-730.
53. OTERO JH, LIZAK B, HENDERSHOT LM (2010) LIFE AND DEATH OF A BIP SUBSTRATE. SEMIN CELL DEV BIOL 21: 472-478.
54. KNITTLER MR, HAAS IG (1992) INTERACTION OF BIP WITH NEWLY SYNTHESIZED IMMUNOGLOBULIN LIGHT CHAIN MOLECULES: CYCLES OF SEQUENTIAL BINDING AND RELEASE. EMBO J 11: 1573-1581.
55. MELNICK J, DUL JL, ARGON Y (1994) SEQUENTIAL INTERACTION OF THE CHAPERONES BIP AND GRP94 WITH IMMUNOGLOBULIN CHAINS IN THE ENDOPLASMIC RETICULUM. NATURE 370: 373-375.
56. LAVERTY D, DESAI R, UCHAŃSKI T, MASIULIS S, STEC WJ, ET AL. (2019) CRYO-EM STRUCTURE OF THE HUMAN A1B3Γ2 GABA(A) RECEPTOR IN A LIPID BILAYER. NATURE 565: 516-520.
57. ZHU S, NOVIELLO CM, TENG J, WALSH RM, JR., KIM JJ, ET AL. (2018) STRUCTURE OF A HUMAN SYNAPTIC GABAA RECEPTOR. NATURE 559: 67-72.
58. NASHMI R, DICKINSON ME, MCKINNEY S, JAREB M, LABARCA C, ET AL. (2003) ASSEMBLY OF ALPHA4BETA2 NICOTINIC ACETYLCHOLINE RECEPTORS ASSESSED WITH FUNCTIONAL FLUORESCENTLY LABELED SUBUNITS: EFFECTS OF LOCALIZATION, TRAFFICKING, AND NICOTINE-INDUCED UPREGULATION IN CLONAL MAMMALIAN CELLS AND IN CULTURED MIDBRAIN NEURONS. J NEUROSCI 23: 11554-11567.
59. GALLAGHER MJ, DING L, MAHESHWARI A, MACDONALD RL (2007) THE GABA(A) RECEPTOR ALPHA 1 SUBUNIT EPILEPSY MUTATION A322D

INHIBITS TRANSMEMBRANE HELIX FORMATION AND CAUSES PROTEASOMAL DEGRADATION. PROC NATL ACAD SCI USA 104: 12999-13004.
60. COSSETTE P, LIU LD, BRISEBOIS K, DONG HH, LORTIE A, ET AL. (2002) MUTATION OF GABRA1 IN AN AUTOSOMAL DOMINANT FORM OF JUVENILE MYOCLONIC EPILEPSY. NAT GENET 31: 184-189.
61. CHANGEUX JP, CHRISTOPOULOS A (2016) ALLOSTERIC MODULATION AS A UNIFYING MECHANISM FOR RECEPTOR FUNCTION AND REGULATION. CELL 166: 1084-1102.
62. NEMECZ A, PREVOST MS, MENNY A, CORRINGER PJ (2016) EMERGING MOLECULAR MECHANISMS OF SIGNAL TRANSDUCTION IN PENTAMERIC LIGAND-GATED ION CHANNELS. NEURON 90: 452-470.
63. MORALES-PEREZ CL, NOVIELLO CM, HIBBS RE (2016) X-RAY STRUCTURE OF THE HUMAN A4B2 NICOTINIC RECEPTOR. NATURE 538: 411-415.
64. NASHMI R, LESTER HA (2006) CNS LOCALIZATION OF NEURONAL NICOTINIC RECEPTORS. J MOL NEUROSCI 30: 181-184.
65. DAU A, KOMAL P, TRUONG M, MORRIS G, EVANS G, ET AL. (2013) RIC-3 DIFFERENTIALLY MODULATES A4B2 AND A7 NICOTINIC RECEPTOR ASSEMBLY, EXPRESSION, AND NICOTINE-INDUCED RECEPTOR UPREGULATION. BMC NEUROSCI 14: 47.
66. SON CD, MOSS FJ, COHEN BN, LESTER HA (2009) NICOTINE NORMALIZES INTRACELLULAR SUBUNIT STOICHIOMETRY OF NICOTINIC RECEPTORS CARRYING MUTATIONS LINKED TO AUTOSOMAL DOMINANT NOCTURNAL FRONTAL LOBE EPILEPSY. MOL PHARMACOL 75: 1137-1148.
67. DAU A, KOMAL P, TRUONG M, MORRIS G, EVANS G, ET AL. (2013) RIC-3 DIFFERENTIALLY MODULATES ALPHA4BETA2 AND ALPHA7 NICOTINIC RECEPTOR ASSEMBLY, EXPRESSION, AND NICOTINE-INDUCED RECEPTOR UPREGULATION. BMC NEUROSCI 14: 47.
68. MILLAR NS (2008) RIC-3: A NICOTINIC ACETYLCHOLINE RECEPTOR CHAPERONE. BRITISH JOURNAL OF PHARMACOLOGY 153: S177-S183.
69. TAYLOR PM, THOMAS P, GORRIE GH, CONNOLLY CN, SMART TG, ET AL. (1999) IDENTIFICATION OF AMINO ACID RESIDUES WITHIN GABA(A) RECEPTOR BETA SUBUNITS THAT MEDIATE BOTH HOMOMERIC AND HETEROMERIC RECEPTOR EXPRESSION. J NEUROSCI 19: 6360-6371.
70. MILLER PS, ARICESCU AR (2014) CRYSTAL STRUCTURE OF A HUMAN GABA RECEPTOR. NATURE 512: 270-275.
71. ONO T, MIYAZAKI T, ISHIDA Y, UEHATA M, NAGATA K (2012) DIRECT IN VITRO AND IN VIVO EVIDENCE FOR INTERACTION BETWEEN HSP47 PROTEIN AND COLLAGEN TRIPLE HELIX. J BIOL CHEM 287: 6810-6818.
72. TASAB M, BATTEN MR, BULLEID NJ (2000) HSP47: A MOLECULAR CHAPERONE THAT INTERACTS WITH AND STABILIZES CORRECTLY-FOLDED PROCOLLAGEN. EMBO J 19: 2204-2211.
73. WIDMER C, GEBAUER JM, BRUNSTEIN E, ROSENBAUM S, ZAUCKE F, ET AL. (2012) MOLECULAR BASIS FOR THE ACTION OF THE COLLAGEN-SPECIFIC CHAPERONE HSP47/SERPINH1 AND ITS STRUCTURE-SPECIFIC CLIENT RECOGNITION. PROC NATL ACAD SCI U S A 109: 13243-13247.

74. ZHOU J, LIU CY, BACK SH, CLARK RL, PEISACH D, ET AL. (2006) THE CRYSTAL STRUCTURE OF HUMAN IRE1 LUMINAL DOMAIN REVEALS A CONSERVED DIMERIZATION INTERFACE REQUIRED FOR ACTIVATION OF THE UNFOLDED PROTEIN RESPONSE. PROC NATL ACAD SCI U S A 103: 14343-14348.
75. EL ACHKAR CM, HARRER M, SMITH L, KELLY M, IQBAL S, ET AL. (2021) CHARACTERIZATION OF THE GABRB2-ASSOCIATED NEURODEVELOPMENTAL DISORDERS. ANN NEUROL 89: 573-586.
76. DI XJ, WANG YJ, COTTER E, WANG M, WHITTSETTE AL, ET AL. (2021) PROTEOSTASIS REGULATORS RESTORE FUNCTION OF EPILEPSY-ASSOCIATED GABA(A) RECEPTORS. CELL CHEM BIOL 28: 46-59 E47.
77. FU YL, HAN DY, WANG YJ, DI XJ, YU HB, ET AL. (2018) REMODELING THE ENDOPLASMIC RETICULUM PROTEOSTASIS NETWORK RESTORES PROTEOSTASIS OF PATHOGENIC GABAA RECEPTORS. PLOS ONE 13: E0207948.
78. HAN DY, DI XJ, FU YL, MU TW (2015) COMBINING VALOSIN-CONTAINING PROTEIN (VCP) INHIBITION AND SUBERANILOHYDROXAMIC ACID (SAHA) TREATMENT ADDITIVELY ENHANCES THE FOLDING, TRAFFICKING, AND FUNCTION OF EPILEPSY-ASSOCIATED GAMMA-AMINOBUTYRIC ACID, TYPE A (GABAA) RECEPTORS. J BIOL CHEM 290: 325-337.
79. HAN DY, GUAN BJ, WANG YJ, HATZOGLOU M, MU TW (2015) L-TYPE CALCIUM CHANNEL BLOCKERS ENHANCE TRAFFICKING AND FUNCTION OF EPILEPSY-ASSOCIATED ALPHA1(D219N) SUBUNITS OF GABA RECEPTORS. ACS CHEM BIOL 10: 2135-2148.
80. WHITTSETTE AL, WANG YJ, MU TW (2022) THE ENDOPLASMIC RETICULUM MEMBRANE COMPLEX PROMOTES PROTEOSTASIS OF GABA(A) RECEPTORS. ISCIENCE 25: 104754.
81. SCHNEIDER CA, RASBAND WS, ELICEIRI KW (2012) NIH IMAGE TO IMAGEJ: 25 YEARS OF IMAGE ANALYSIS. NAT METHODS 9: 671-675.
82. MOSS FJ, IMOUKHUEDE PI, SCOTT K, HU J, JANKOWSKY JL, ET AL. (2009) GABA TRANSPORTER FUNCTION, OLIGOMERIZATION STATE, AND ANCHORING: CORRELATES WITH SUBCELLULARLY RESOLVED FRET. J GEN PHYSIOL 134: 489-521.
83. FEIGE JN, SAGE D, WAHLI W, DESVERGNE B, GELMAN L (2005) PIXFRET, AN IMAGEJ PLUG-IN FOR FRET CALCULATION THAT CAN ACCOMMODATE VARIATIONS IN SPECTRAL BLEED-THROUGHS. MICROSC RES TECH 68: 51-58.
84. ELANGOVAN M, WALLRABE H, CHEN Y, DAY RN, BARROSO M, ET AL. (2003) CHARACTERIZATION OF ONE- AND TWO-PHOTON EXCITATION FLUORESCENCE RESONANCE ENERGY TRANSFER MICROSCOPY. METHODS 29: 58-73.
85. HENDERSON BJ, WALL TR, HENLEY BM, KIM CH, NICHOLS WA, ET AL. (2016) MENTHOL ALONE UPREGULATES MIDBRAIN NACHRS, ALTERS NACHR SUBTYPE STOICHIOMETRY, ALTERS DOPAMINE NEURON FIRING

FREQUENCY, AND PREVENTS NICOTINE REWARD. J NEUROSCI 36: 2957-2974.

FIGURE LEGENDS

Figure 1. Hsp47 interacts with $GABA_A$ receptors. (**A**) Endogenous interactions between $GABA_A$ receptor α1 subunits and Hsp47. Mouse brain homogenates from 8-10 weeks C57BL/6J mice were immunoprecipitated with an anti-α1 antibody, and the immunoisolated eluents were blotted with indicated antibodies (n = 3). IgG was included as a negative control for non-specific binding. (**B**) Recombinant Hsp47 binds recombinant α1 subunit and β2 subunit of $GABA_A$ receptors *in vitro*. GST, GST-tagged α1 or GST-tagged β2 recombinant protein was mixed with His-tagged Hsp47 in buffers containing 1% Triton X-100. The protein complex was isolated by immunoprecipitation using an anti-His antibody, and the immunopurified eluents were separated by SDS-PAGE and blotted with indicated antibodies (n = 3). (**C**) MicroScale Thermophoresis (MST) was used to determine the binding affinities between ER luminal chaperones (Hsp47 and BiP) to RED-labeled His-α1(ERD). Increasing concentrations of recombinant Hsp47 or BiP proteins (0.20 nM – 10 μM) were incubated with 50 nM RED-labeled His-α1(ERD) protein in PBS with Tween-20 (0.05%) (n = 3). Then samples were loaded to the capillaries and measured using a Monolith NT.115 instrument with the settings of 40% LED/excitation and 40% MST power. The data were analyzed using the Monolith software for the calculation of the dissociation constant (Kd). IP, immunoprecipitation; IB, immunoblotting.

Figure 2. Hsp47 positively regulates the surface expression of endogenous $GABA_A$ receptors in cultured neurons. (**A**) Effect of Hsp47 on the surface expression of endogenous $GABA_A$ receptor subunits in primary rat hippocampal neurons. Cultured neurons were transduced with Hsp47 siRNA lentivirus or scrambled siRNA lentivirus at days *in vitro* (DIV) 10. Forty-eight hours post

transduction, surface $GABA_A$ receptors were stained using anti-α1 subunit or anti-β2/β3 subunit antibodies without membrane permeabilization. The cells were then washed, and permeabilized before we stained the nuclei with DAPI. At least 20 neurons from at least three transductions were imaged by confocal microscopy for each condition. Representative images are shown on the left side of panel A. Scale bar = 10 μm. Quantification of the fluorescence intensity of the surface $GABA_A$ receptor subunits after background correction was shown on the right. (**B**) Whole-cell patch clamping was performed to record GABA-induced currents. Neurons were subjected to transduction as in (**A**). The recordings were carried out 48 hours post transduction. Representative traces are shown in the left-hand panel. Peak current amplitude (I_{max}) is shown on the right (n = 10). The holding potential was set at −60 mV. pA: picoampere. Each data point is reported as mean ± SD. Statistical significance was calculated using an unpaired two-tailed Student's t-Test. *** $p < 0.001$.

Figure 3. Hsp47 preferentially binds the folded conformation of $GABA_A$ receptor subunits. (**A**) Overexpression of Hsp47 increases the endo H-resistant post-ER glycoform of the α1 subunit in HEK293T cells stably expressing α1β2γ2 $GABA_A$ receptors. PNGase F treatment serves as a control for unglycosylated α1 subunit (lane 5). Two endo H-resistant bands were detected for the α1 subunit, indicated by the bracket (lanes 2 and 4). Quantification of the ratio of endo H-resistant / total α1 subunit bands, as a measure of the ER-to-Golgi trafficking efficiency, is shown on the bottom (n = 3). (**B**) Dithiothreitol (DTT) treatment decreases the interaction between Hsp47 and α1 subunit of $GABA_A$ receptors. HEK293T cells stably expressing WT α1β2γ2 $GABA_A$ receptors were treated with indicated concentration of DTT in the PBS buffer

for 10 minutes. Then Triton X-100 cell extracts were immunoprecipitated with a mouse anti-Hsp47 antibody, and the immunoisolated eluents were subjected for immunoblotting assay (n = 3). Quantification of the relative intensity of α1/Hsp47 post IP, as a measure of their interactions, is shown on the bottom panel. (**C**) Disulfide bond mutations in the α1 subunit decrease the interaction between Hsp47 and α1 subunit of $GABA_A$ receptors. HEK293T cells were transiently transfected with WT α1β2γ2, α1(C166A)β2γ2, or α1(C166A, C180A)β2γ2 subunits. Forty-eight hours post transfection, Triton X-100 cell extracts were immunoprecipitated with a mouse anti-Hsp47 antibody, and the immunoisolated eluents were subjected for immunoblotting assay (n = 3). Quantification of the relative intensity of α1/Hsp47 post IP is shown on the bottom panel. (**D**) Disulfide bond mutations in the α1 subunits decrease the solubility of the α1 subunit protein. HEK293T cells were transiently transfected as in (**C**). Forty-eight hours post transfection, the Triton X-100 detergent soluble fractions and the Triton X-100 detergent insoluble fractions were isolated for immunoblotting assay (n = 3). Quantification of the ratio of insoluble/soluble fractions, as a measure of relative aggregation, is shown on the bottom panel. (**E**) DTT treatment increases the interaction between BiP and α1 subunit of $GABA_A$ receptors. HEK293T cells stably expressing α1β2γ2 $GABA_A$ receptors were treated with indicated concentrations of DTT in PBS for 10 minutes. Then Triton X-100 cell extracts were immunoprecipitated with a mouse anti-α1 antibody, and the immunoisolated eluents were subjected for immunoblotting assay (n = 3). Quantification of the relative intensity of BiP/α1 post IP is shown on the bottom panel. (**F**) The disulfide mutations of α1 subunit increase the interaction between BiP and the α1 subunit. HEK293T cells were transiently transfected as in (**C**). Forty-eight hours post transfection, Triton X-100 cell extracts were immunoprecipitated with a mouse anti-α1 antibody, and the

immunoisolated eluents were subjected for immunoblotting assay (n = 3). Quantification of the relative intensity of BiP/α1 post IP is shown on the bottom panel. IP, immunoprecipitation; IB, immunoblotting. Each data point is reported as mean ± SD. Significant difference was analyzed by t-test (**A**), or a one-way ANOVA followed by post hoc Tukey's HSD test (**B-F**). *, $p < 0.05$; **, $p < 0.01$; ***, $p < 0.001$.

Figure 4. Hsp47 promotes the assembly of $GABA_A$ receptors. (**A**) Hsp47 overexpression increases FRET efficiency between CFP-tagged α1 subunit and YFP-tagged β2 subunit of $GABA_A$ receptors. HEK293T cells were transfected with CFP-tagged α1 subunit, YFP-tagged β2 subunit, and γ2 subunit; in addition, cells were transfected with empty vector (EV) control or Hsp47 cDNA. Forty-eight hours post transfection, pixel-based FRET was used to measure the FRET efficiency between α1-CFP and β2-YFP by using a confocal microscope. Representative images were shown for the CFP channel (1st columns), YFP channel (2nd columns), and FRET efficiency (3rd columns). Scale bar = 10 μm. Quantification of the FRET efficiency from 30-41 cells was achieved using the ImageJ PixFRET plug-in, and shown on the right. (**B**) Overexpression of Hsp47 increases the interaction between α1 and β2 subunit of $GABA_A$ receptors. HEK293T cells stably expressing α1(Flag-β2)γ2 $GABA_A$ receptors were transfected with empty vector (EV) control or Hsp47 cDNA. Forty-eight hours post transfection, Triton X-100 cell extracts were immunoprecipitated with a mouse anti-α1 antibody, and the immunoisolated eluents were subjected to immunoblotting assay. Quantification of the relative intensity of Flag-β2 / α1 post IP is shown on the bottom (n = 3). (**C**) HEK293T cells were transiently transfected with empty vector (EV), α1 subunits alone, or both α1 and β2 subunits of

$GABA_A$ receptors together with Hsp47 cDNA plasmids at various concentrations. Forty-eight hours post transfection, cells were lysed in RIPA buffer, and the total cell lysates were subjected to SDS-PAGE under non-reducing conditions and reducing conditions and immunoblotting analysis. (**D**) Quantification of the 480 kDa band intensities for α1 and β2 subunits under non-reducing conditions (lanes 2-5 in **C**) (n = 3). (**E**) Quantification of the 50 kDa band intensities for α1 and β2 subunits under reducing conditions (lanes 7-10 in **C**) (n = 3). IP, immunoprecipitation; IB, immunoblotting. Each data point is reported as mean ± SD. Significant difference was analyzed by t-test (**A**, **B**) or a one-way ANOVA followed by post hoc Tukey's HSD test (**D**, **E**). *, $p < 0.05$; **, $p < 0.01$; ***, $p < 0.001$.

Figure 5. Hsp47 positively regulates the functional surface expression of epilepsy-associated $GABA_A$ receptors carrying the α1(A322D) variant. (**A**) Overexpression of Hsp47 increases the endo H-resistant post-ER glycoform of the α1 subunit in HEK293T cells expressing α1(A322D)β2γ2 $GABA_A$ receptors. PNGase F treatment serves as a control for unglycosylated α1 subunit (lane 5). Two endo H-resistant bands were detected for the α1 subunit, indicated by the bracket (lanes 2 and 4). Quantification of the ratio of endo H-resistant / total α1 subunit bands, as a measure of the ER-to-Golgi trafficking efficiency, is shown on the bottom (n = 3). (**B**) HEK293T cells expressing α1(A322D)β2γ2 $GABA_A$ receptors were transfected with empty vector (EV) control or Hsp47 cDNA plasmids. Forty-eight hours post transfection, the surface proteins were measured using a cell surface protein biotinylation assay. The Na^+/K^+ ATPase serves as a loading control for biotinylated membrane proteins. Surface α1 subunit intensities were quantified using ImageJ and shown on the bottom (n = 3). Alternatively, cells were lysed,

and the total cell lysates were subjected to SDS-PAGE and immunoblotted for Hsp47. β-actin serves as a total protein loading control. (**C**) Whole-cell patch clamping was performed to record GABA-induced currents. HEK293T cells were treated as in (**B**). The recording was carried out 48 hours post transfection. The holding potential was set at -60 mV. Representative traces were shown. Quantification of the peak currents (I_{max}) from 17-20 cells is shown on the bottom. pA: picoampere. Each data point is reported as mean ± SD. Statistical significance was calculated using two-tailed Student's t-Test. *, $p < 0.05$; **, $p < 0.01$; ***, $p < 0.001$.

Figure 6. Hsp47 promotes the assembly and function of α4β2 nicotinic acetylcholine receptors (nAChRs). (**A**) Hsp47 overexpression increases FRET efficiency between CFP-tagged β2 subunit and YFP-tagged α4 subunit of nAChRs. HEK293T cells were transfected with CFP-tagged β2 subunit and YFP-tagged α4 subunit; in addition, cells were transfected with empty vector (EV) control or Hsp47 cDNA. Forty-eight hours post transfection, pixel-based FRET was used to measure the FRET efficiency between β2-CFP and α4-YFP by using a confocal microscope. Representative images were shown for the CFP channel (1st columns), YFP channel (2nd columns), and FRET efficiency (3rd columns). Scale bar = 10 μm. Quantification of the FRET efficiency from 60-70 cells was achieved using the ImageJ PixFRET plug-in, and shown on the right. (**B**) HEK293T cells were transfected with CFP-tagged β2 subunit and YFP-tagged α4 subunit of nAChRs; in addition, cells were transfected with empty vector (EV) control or Hsp47 cDNA. Forty-eight hours post transfection, whole-cell patch clamping was performed to record nicotine-induced currents. Representative traces were shown. Quantification of the peak currents (I_{max}) from 9 cells is shown on the right. The holding potential was set at -60 mV. pA:

picoampere. Each data point is reported as mean ± SD. Statistical significance was calculated using two-tailed Student's t-Test. * $p < 0.05$; *** $p < 0.001$.

Figure 7. Proposed mechanism of Hsp47 in the assembly of $GABA_A$ receptors. BiP and calnexin assist the subunit folding early in the ER lumen. Hsp47 operates after BiP and binds the folded states of the α1 or β subunits in the ER lumen. Hsp47 links the α1 and β subunits and promotes their inter-subunit interactions. As a result, Hsp47 promotes the formation of assembly intermediates and the native pentameric receptors in the ER. Assembled receptors will traffic to the Golgi and onward to the plasma membrane for function.

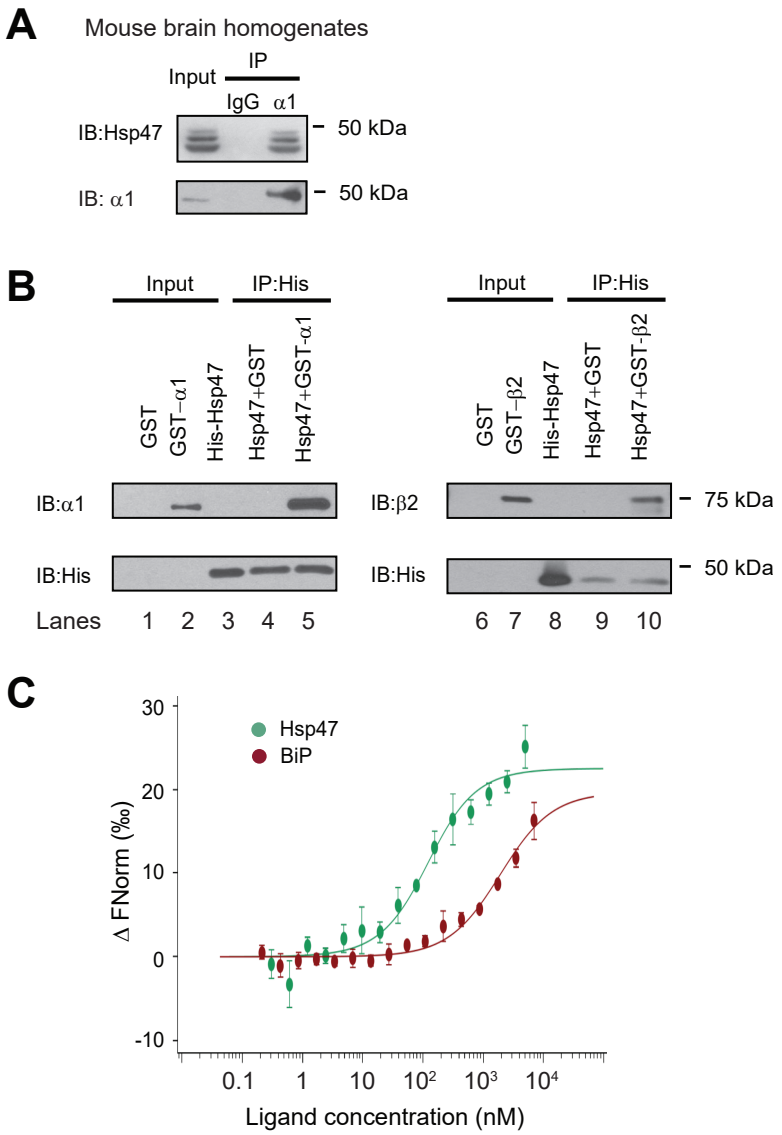
A
Mouse brain homogenates
Input
IP
IgG
α1
IB:Hsp47
50 kDa
IB: α1
50 kDa
B
Input
IP:His
GST
GST−α1
His-Hsp47
Hsp47+GST
Hsp47+GST-α1
IB:α1
IB:His
Input
IP:His
GST
GST−β2
His-Hsp47
Hsp47+GST
Hsp47+GST-β2
IB:β2
IB:His
75 kDa
50 kDa
Lanes 1 2 3 4 5 6 7 8 9 10
C
Hsp47
BiP
Δ FNorm (‰)
30
20
10
0
-10
0.1
1
10
10²
10³
10⁴
Ligand concentration (nM)

Figure 1

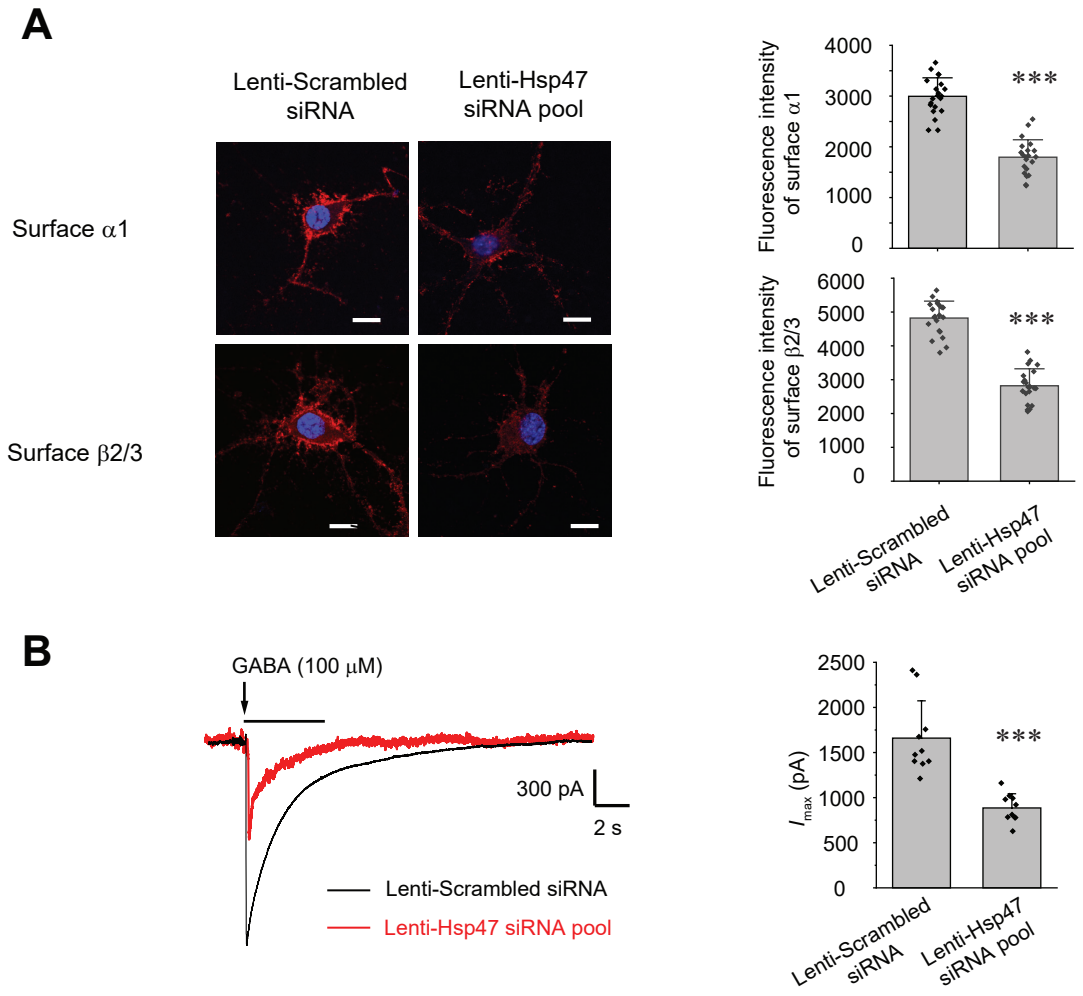
A
Lenti-Scrambled siRNA
Lenti-Hsp47 siRNA pool
Surface α1
Surface β2/3
Fluorescence intensity of surface α1
Fluorescence intensity of surface β2/3
4000
3000
2000
1000
0
6000
5000
4000
3000
2000
1000
0
***
***
Lenti-Scrambled siRNA
Lenti-Hsp47 siRNA pool
B
GABA (100 μM)
300 pA
2 s
Lenti-Scrambled siRNA
Lenti-Hsp47 siRNA pool
I_{max} (pA)
2500
2000
1500
1000
500
0
***
Lenti-Scrambled siRNA
Lenti-Hsp47 siRNA pool

Figure 2

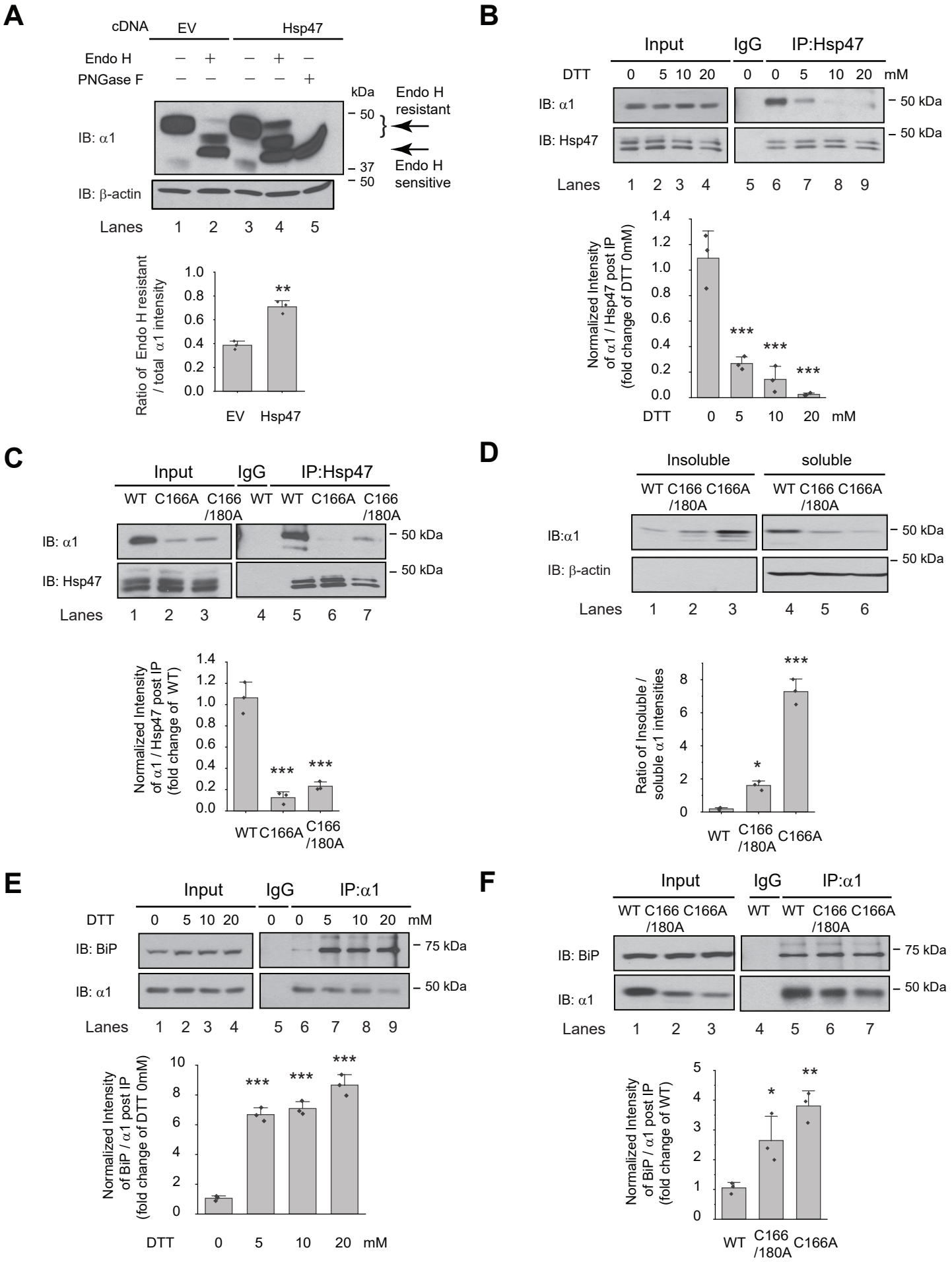
A
cDNA
EV
Hsp47
Endo H
PNGase F
kDa
Endo H resistant
IB: α1
50
37
50
Endo H sensitive
IB: β-actin
Lanes 1 2 3 4 5
Ratio of Endo H resistant / total α1 intensity
EV
Hsp47
B
Input
IgG
IP:Hsp47
DTT 0 5 10 20 0 0 5 10 20 mM
IB: α1
IB: Hsp47
50 kDa
Lanes 1 2 3 4 5 6 7 8 9
Normalized Intensity of α1 / Hsp47 post IP (fold change of DTT 0mM)
DTT 0 5 10 20 mM
C
Input
IgG
IP:Hsp47
WT C166A C166 /180A WT WT C166A C166 /180A
IB: α1
IB: Hsp47
50 kDa
Lanes 1 2 3 4 5 6 7
Normalized Intensity of α1 / Hsp47 post IP (fold change of WT)
WT C166A C166 /180A
D
Insoluble
soluble
WT C166 C166A /180A
IB:α1
IB: β-actin
50 kDa
Lanes 1 2 3 4 5 6
Ratio of Insoluble / soluble α1 intensities
WT C166 /180A C166A
E
Input
IgG
IP:α1
DTT 0 5 10 20 0 0 5 10 20 mM
IB: BiP
IB: α1
75 kDa
50 kDa
Lanes 1 2 3 4 5 6 7 8 9
Normalized Intensity of BiP / α1 post IP (fold change of DTT 0mM)
DTT 0 5 10 20 mM
F
Input
IgG
IP:α1
WT C166 C166A /180A WT WT C166 C166A /180A
IB: BiP
IB: α1
75 kDa
50 kDa
Lanes 1 2 3 4 5 6 7
Normalized Intensity of BiP / α1 post IP (fold change of WT)
WT C166 /180A C166A

Figure 3

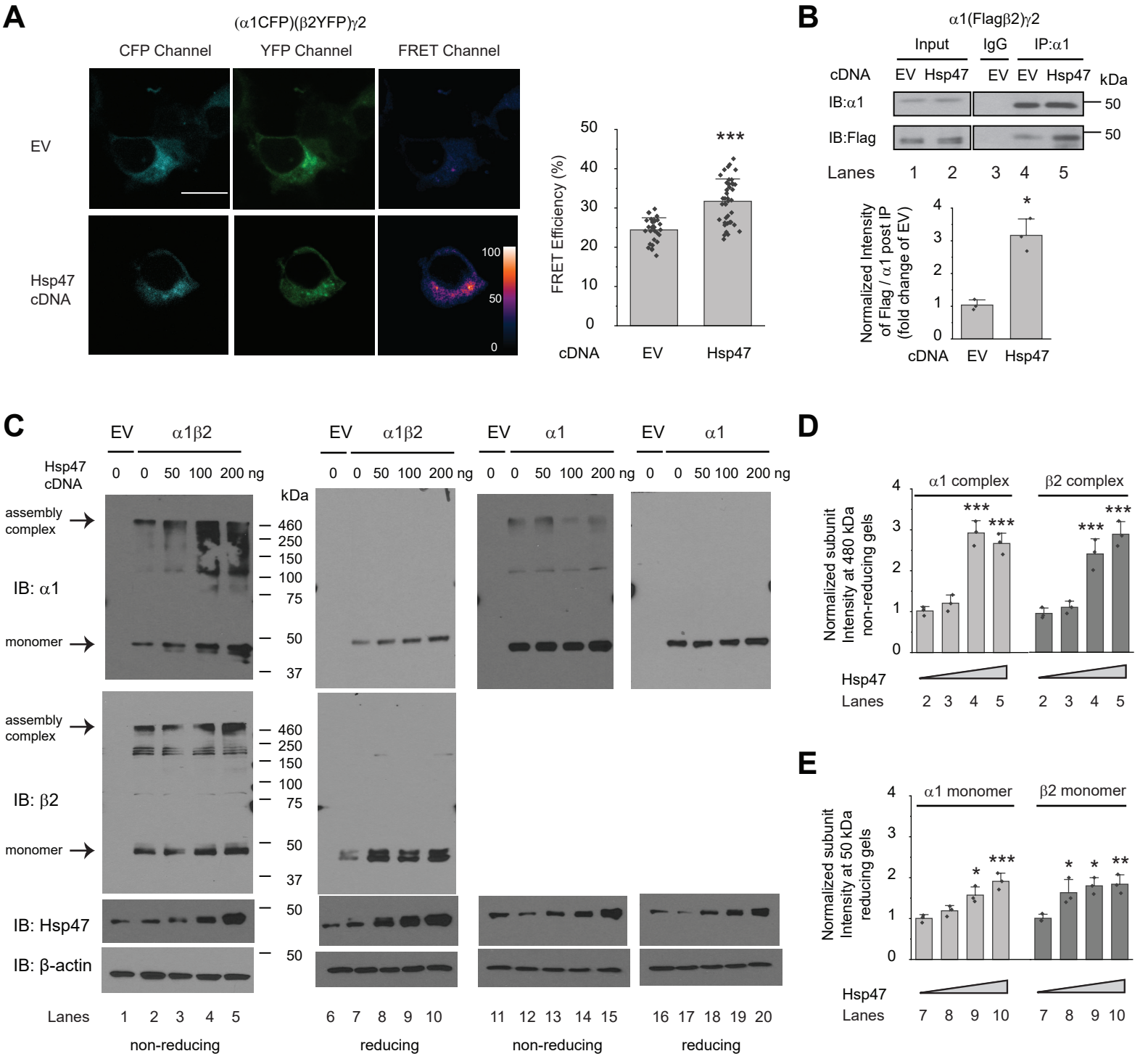
A
(α1CFP)(β2YFP)γ2
CFP Channel
YFP Channel
FRET Channel
EV
Hsp47 cDNA
100
50
0
FRET Efficiency (%)
50
40
30
20
10
0
***
cDNA
EV
Hsp47
B
α1(Flagβ2)γ2
Input
IgG
IP:α1
cDNA
EV
Hsp47
EV
EV
Hsp47
kDa
IB:α1
IB:Flag
50
50
Lanes
1
2
3
4
5
Normalized Intensity of Flag / α1 post IP (fold change of EV)
4
3
2
1
0
*
cDNA
EV
Hsp47
C
EV
α1β2
EV
α1β2
EV
α1
EV
α1
Hsp47 cDNA
0
0
50
100
200 ng
kDa
assembly complex
IB: α1
monomer
460
250
150
100
75
50
37
assembly complex
IB: β2
monomer
IB: Hsp47
IB: β-actin
Lanes
1 2 3 4 5
6 7 8 9 10
11 12 13 14 15
16 17 18 19 20
non-reducing
reducing
non-reducing
reducing
D
α1 complex
β2 complex
Normalized subunit Intensity at 480 kDa non-reducing gels
***
Hsp47
Lanes
2 3 4 5
2 3 4 5
E
α1 monomer
β2 monomer
Normalized subunit Intensity at 50 kDa reducing gels
*
***
**
Hsp47
Lanes
7 8 9 10
7 8 9 10

Figure 4

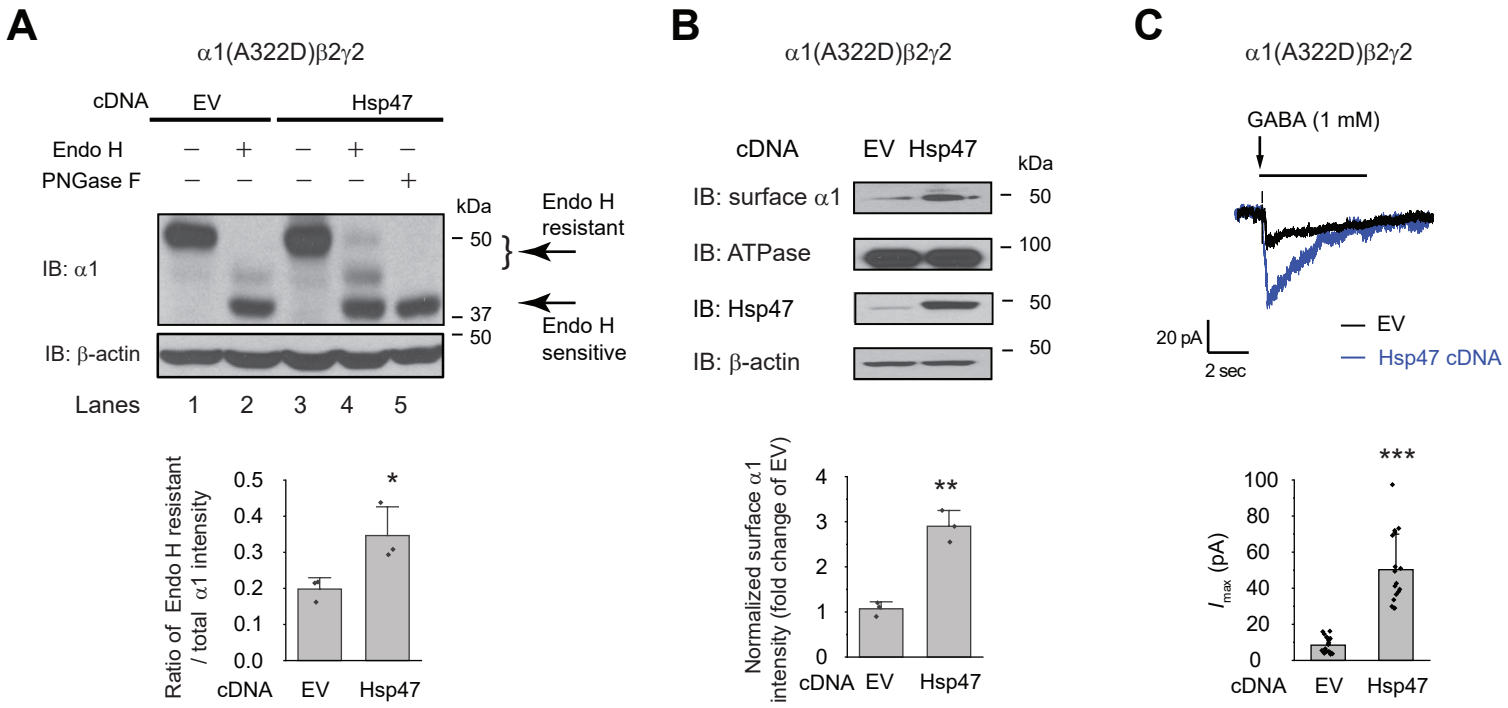
A
α1(A322D)β2γ2
cDNA
EV
Hsp47
Endo H
PNGase F
kDa
Endo H resistant
IB: α1
50
37
50
Endo H sensitive
IB: β-actin
Lanes
1 2 3 4 5
Ratio of Endo H resistant / total α1 intensity
0.5
0.4
0.3
0.2
0.1
0.0
*
cDNA EV Hsp47
B
α1(A322D)β2γ2
cDNA EV Hsp47
kDa
IB: surface α1
IB: ATPase
IB: Hsp47
IB: β-actin
50
100
50
50
Normalized surface α1 intensity (fold change of EV)
4
3
2
1
0
**
cDNA EV Hsp47
C
α1(A322D)β2γ2
GABA (1 mM)
20 pA
2 sec
EV
Hsp47 cDNA
I_{max} (pA)
100
80
60
40
20
0
***
cDNA EV Hsp47

Figure 5

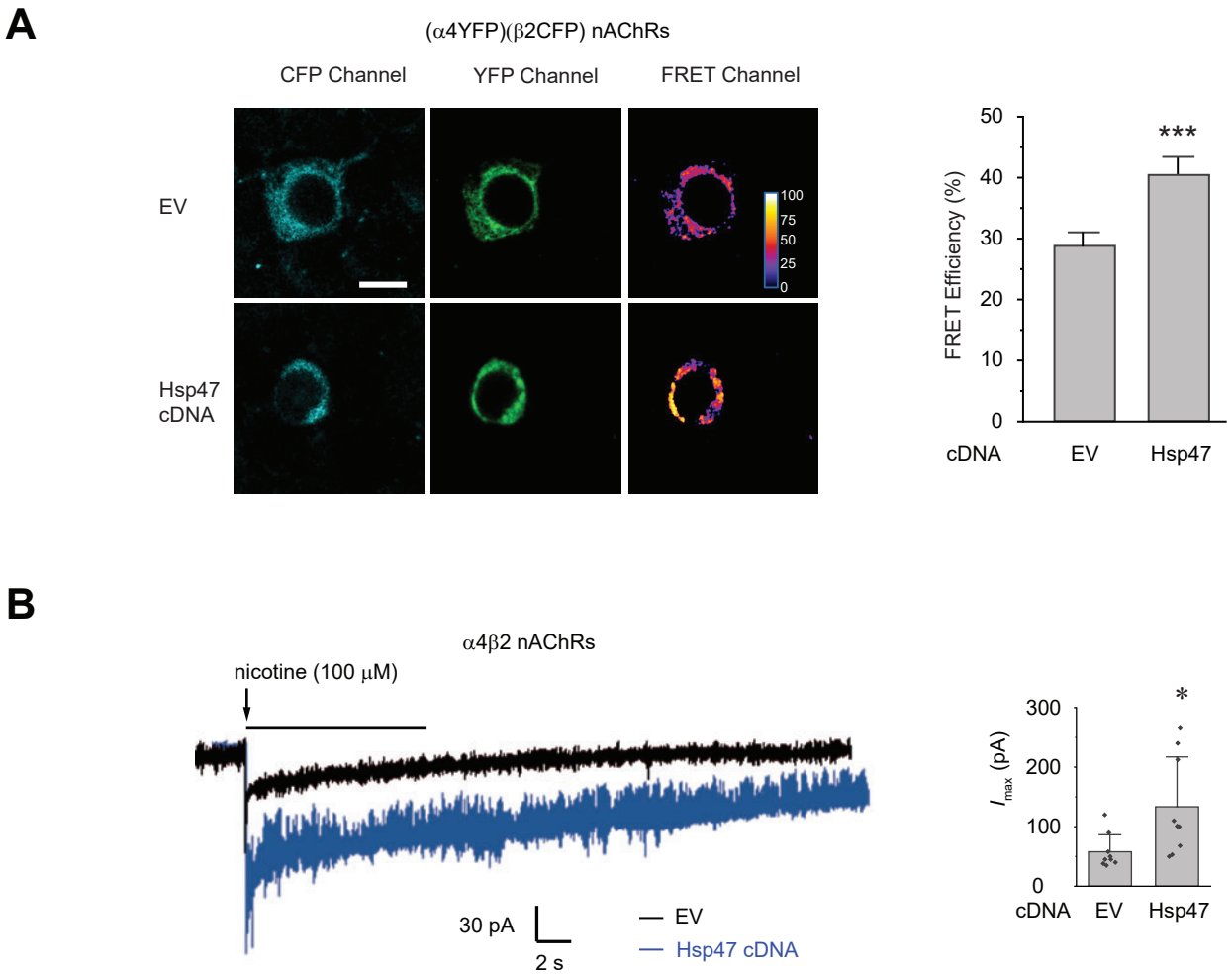
A
(α4YFP)(β2CFP) nAChRs
CFP Channel
YFP Channel
FRET Channel
EV
Hsp47 cDNA
100
75
50
25
0
FRET Efficiency (%)
50
40
30
20
10
0
***
cDNA
EV
Hsp47
B
α4β2 nAChRs
nicotine (100 μM)
30 pA
2 s
EV
Hsp47 cDNA
I_{max} (pA)
300
200
100
0
*
cDNA
EV
Hsp47

Figure 6

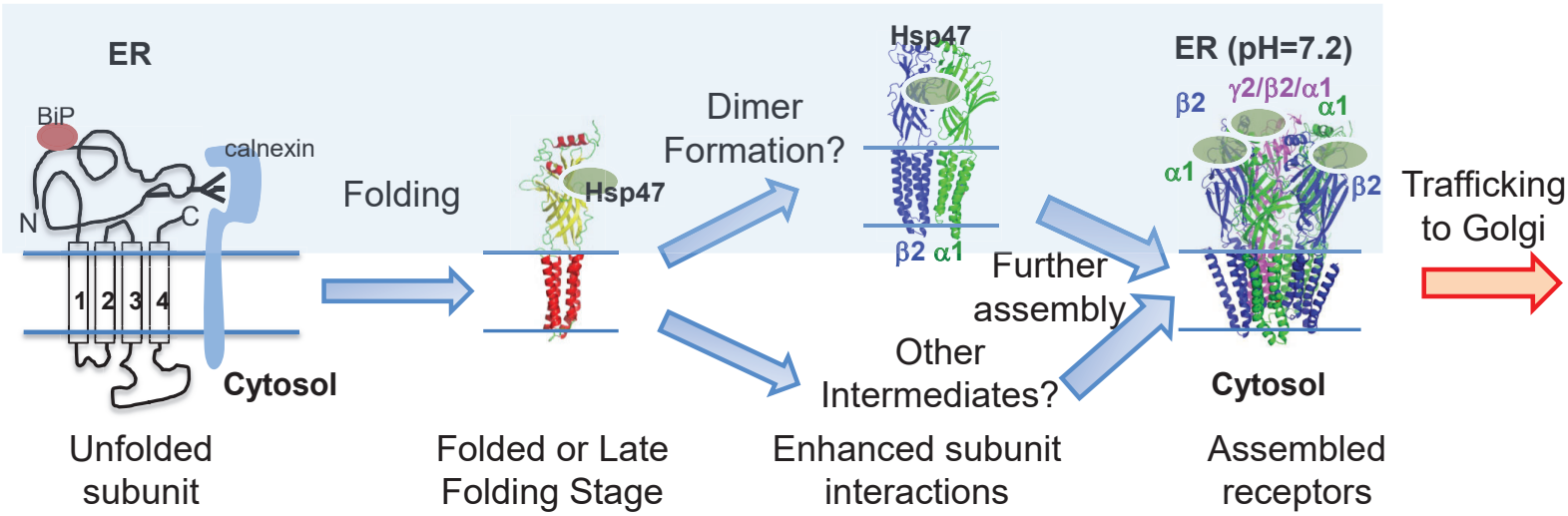
ER
BiP
calnexin
N
C
1
2
3
4
Cytosol
Folding
Hsp47
Dimer
Formation?
Hsp47
β2 α1
Further
assembly
Other
Intermediates?
ER (pH=7.2)
β2
γ2/β2/α1
α1
α1
β2
Cytosol
Trafficking
to Golgi
Unfolded
subunit
Folded or Late
Folding Stage
Enhanced subunit
interactions
Assembled
receptors

Figure 7